10802–10819 *Nucleic Acids Research, 2020, Vol. 48, No. 19* *Published online 30 September 2020*
doi: 10.1093/nar/gkaa798

Rewiring of growth-dependent transcription regulation by a point mutation in region 1.1 of the housekeeping σ factor

Philipp Pletnev[1,2], Danil Pupov[3], Lizaveta Pshanichnaya[1], Daria Esyunina[3], Ivan Petushkov[3], Mikhail Nesterchuk[4], Ilya Osterman[1,4], Maria Rubtsova[1,4], Andrey Mardanov[5], Nikolai Ravin[5], Petr Sergiev[1,4,6,7,*], Andrey Kulbachinskiy[3,*] and Olga Dontsova[1,2,4,6]

[1]Department of Chemistry, Lomonosov Moscow State University, Moscow 119992, Russia, [2]Shemyakin-Ovchinnikov Institute of Bioorganic Chemistry, Moscow 117997, Russia, [3]Institute of Molecular Genetics, Russian Academy of Sciences, Moscow,123182, Russia, [4]Skolkovo Institute of Science and Technology, Skolkovo, Moscow Region 143028, Russia, [5]Institute of Bioengineering, Research Center of Biotechnology of the Russian Academy of Sciences, Moscow, Russia, [6]Belozersky Institute of Physico-Chemical Biology, Lomonosov Moscow State University, Moscow 119992, Russia and [7]Institute of Functional Genomics, Lomonosov Moscow State University, Moscow 119992, Russia

Received November 14, 2019; Revised September 09, 2020; Editorial Decision September 10, 2020; Accepted September 12, 2020

ABSTRACT

In bacteria, rapid adaptation to changing environmental conditions depends on the interplay between housekeeping and alternative σ factors, responsible for transcription of specific regulons by RNA polymerase (RNAP). In comparison with alternative σ factors, primary σs contain poorly conserved region 1.1, whose functions in transcription are only partially understood. We found that a single mutation in region 1.1 in *Escherichia coli* σ^{70} rewires transcription regulation during cell growth resulting in profound phenotypic changes. Despite its destabilizing effect on promoter complexes, this mutation increases the activity of rRNA promoters and also decreases RNAP sensitivity to the major regulator of stringent response DksA. Using total RNA sequencing combined with single-cell analysis of gene expression we showed that changes in region 1.1 disrupt the balance between the "greed" and "fear" strategies thus making the cells more susceptible to environmental threats and antibiotics. Our results reveal an unexpected role of σ region 1.1 in growth-dependent transcription regulation and suggest that changes in this region may facilitate rapid switching of RNAP properties in evolving bacterial populations.

INTRODUCTION

Transcription initiation in bacterial cells is accomplished by the holoenzyme of RNA polymerase (RNAP) consisting of the catalytically active core enzyme and a specificity factor, the σ subunit (1). In addition to the primary σ subunit involved in transcription of housekeeping genes, most bacteria encode alternative σ factors involved in transcription of regulons responsible for adaptation to various growth conditions. All primary σ subunits contain four evolutionary conserved regions, which have distinct functions in transcription initiation (1). Regions σ2 and σ4 recognize the −10 and −35 promoter elements, respectively. A flexible linker formed by region σ3 (subregion σ3.2 or 'σ finger') directly interacts with the template promoter strand upstream of the transcription start site and participates in RNA priming and promoter escape by RNAP (2–4). Region σ1 consists of two parts, σ1.1 and σ1.2. Region σ1.2 is highly conserved in primary σ factors and participates in interactions with core RNAP and with the discriminator element in promoters (4–8). Region 1.1 is poorly conserved but contains a large number of negatively charged residues (Figure 1A) (1,9–12).

The functions of region 1.1 in transcription are poorly understood. In free σ subunit, it interacts with the promoter recognition regions 2 and 4, stabilizes an inactive conformation of σ and inhibits DNA binding, while its deletion stimulates interactions of σ^{70} with promoter sequences (13–16). In addition, region 1.1 has been implicated in holoenzyme assembly, promoter complex forma-

*To whom correspondence should be addressed. Tel: +7 499 1960015; Fax: +7 499 1960015; Email: avkulb@yandex.ru
Correspondence may also be addressed to Petr Sergiev. Tel: +7 495 9395418; Fax: +7 495 9393181; Email: petya@genebee.msu.ru

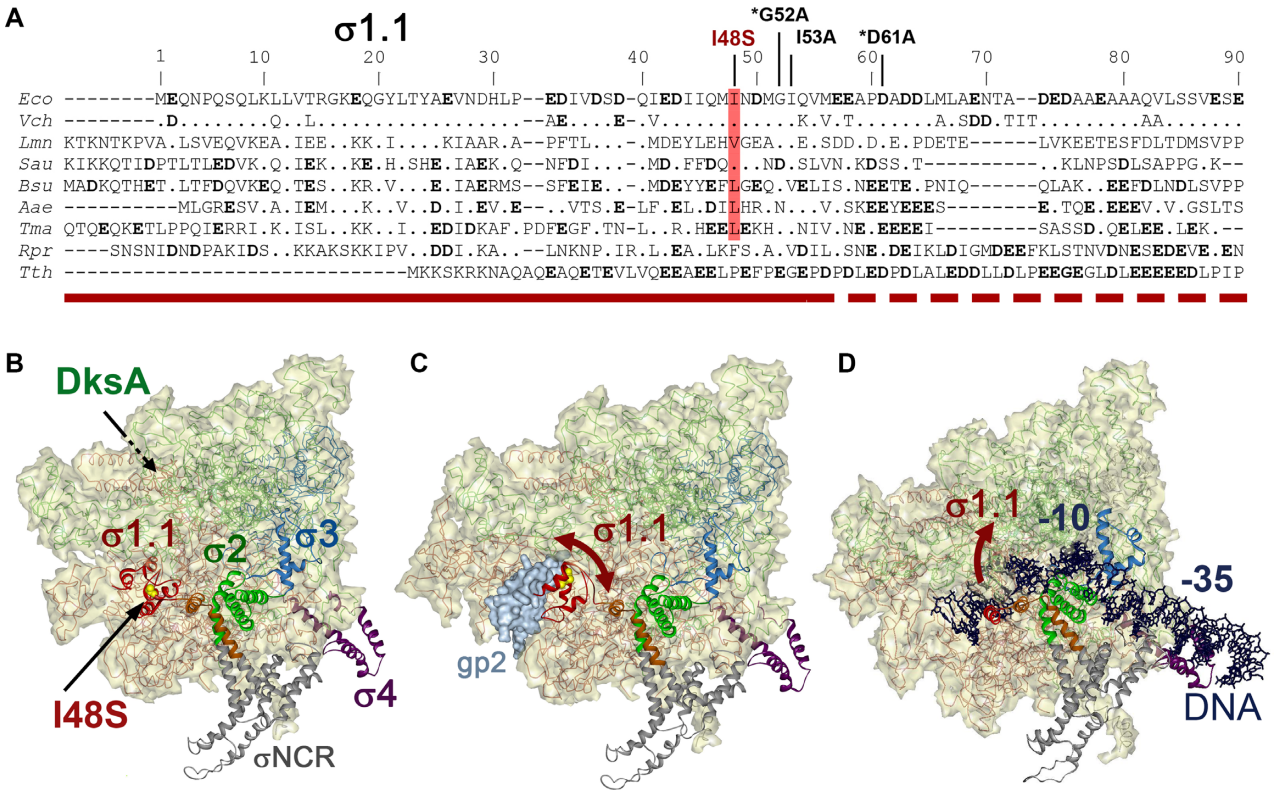

Figure 1. Structure of σ region 1.1 and its possible role in transcription. (**A**) Sequences of region 1.1 in the primary σ subunits from various bacteria (*Eco, Escherichia coli*; *Vch*, *Vibrio cholerae*; *Lmn*, *Listeria monocytogenes*; *Sau*, *Staphylococcus aureus*; *Bsu*, *Bacillus subtilis*; *Aae*, *Aquifex aeolicus*; *Tma*, *Thermotoga maritima*; *Rpr*, *Rickettsia prowazekii*; *Tth*, *Thermus thermophilus*). Identical amino acid residues in different σ subunits are shown with dots; gaps are shown with hyphens. Locations of the N-terminal α-helical domain and nonstructured linker in region 1.1 are indicated below the alignment with solid and dotted lines, respectively. Positions of previously studied substitutions in region 1.1 in *E. coli* σ^{70} are indicated. (**B** and **C**) Structures of the *E. coli* σ^{70} RNAP holoenzyme in free form (4LK1) and in complex with the gp2 protein (light blue) of phage T7 (4LLG, (21)). (**D**) Structure of the open promoter complex of *E. coli* RNAP with a synthetic bubble promoter (4YLN, (25)). RNAP core enzyme is shown as a semi-transparent surface and σ^{70} as a ribbon model. σ^{70} regions are colored as follows: σ1.1, red; σ1.2, orange; σNCR (nonconserved region), gray; σ2, green; σ3, blue; σ4, violet; position of the I48S substitution is shown in yellow. Movements of σ region 1.1 are shown with red arrows (in the open promoter complex structure, region 1.1 is not visible but is located outside of the DNA binding cleft). The site of DksA binding in the secondary channel of RNAP is shown with a dotted arrow. Promoter DNA is dark blue; the −10 and −35 elements are indicated.

tion (12,17–20) and interactions with regulatory bacteriophage proteins (21). FRET measurements demonstrated that σ1.1 is located within the downstream part of the DNA binding cleft in the RNAP holoenzyme but is moved outside upon promoter DNA binding (22,23). Recent structural studies directly visualized positioning of region 1.1 in the DNA binding cleft in free holoenzyme (Figure 1B), which is incompatible with downstream DNA binding in the open promoter complex (Figure 1D) (21,24,25). Furthermore, the conformation of this region is changed upon binding of an inhibitory protein gp2 of phage T7, thus preventing promoter DNA binding (Figure 1C) (21). Single amino acid substitutions in region 1.1 in *E. coli* σ^{70} (Figure 1A) impaired formation of promoter complexes (I53A, (19)) or decreased their stability (G52A and D61A, (12)). Substitution D61A also caused σ^{70} thermolability (12). On the other hand, region 1.1 was shown to destabilize the open promoter complex and determine species-specific variations in promoter complex stabilities, likely by modulating the binding of the nontemplate DNA strand and the downstream promoter duplex by RNAP holoenzyme (20,26). Yet, region 1.1 is not well conserved in primary σ factors and is absent in most alternative σs suggesting that it is not essential for transcription initiation.

In this work, we demonstrate that a point mutation in region 1.1 in *E. coli* σ^{70}, I48S (Figure 1), has profound effects on gene transcription and cell physiology *in vivo* and significantly changes RNAP activity and its sensitivity to regulatory factors *in vitro*. Furthermore, the mutation decreases formation of dormant cells in bacterial populations and thus increases their sensitivity to antibiotics. The results suggest that amino acid substitutions in region σ1.1 can modulate RNAP response to transcription regulators and may drive rapid evolution of RNAP properties in bacteria.

MATERIALS AND METHODS

Strains

Strains used in this work were created on the basis of *E. coli* K12 strain BW25113 using RED-mediated recombination. The cells containing the pKD46 plasmid (27) were induced by 10 mM arabinose for expression of lambda RED genes and transformed with a linear PCR product encoding either

wild-type or I48S σ^{70} and chloramphenicol acetyltransferase. The 5′-end of the PCR product was complementary to the coding region of *rpoD*, while the 3′-end was complementary to the non-coding DNA region downstream of the *rpoD* gene, thus both WT and I48S strains were carrying a chloramphenicol resistance cassette. The pKD46 plasmid was cured by growth at 37°C. The strains were verified by PCR and sequencing.

Analysis of cell fitness

For the measurement of growth curves, LB or MOPS minimal medium was inoculated by a single colony of either the wild-type or I48S strains and incubated for 24 h at 37°C. The culture was diluted to $OD_{600} = 0.01$ (final culture volume of 300 μl) with fresh LB or MOPS minimal medium and grown at 37°C for 12 h in 24-well microtiter plates with constant shaking at 200 rpm. The OD of culture was measured every 40 min. MOPS minimal medium (pH 7.2) was supplemented with glucose (0.2%) in all experiments; 20 amino acids (20 mg/L each) were added when indicated. To examine cell survival in the stationary phase, WT and I48S cells were grown separately in LB medium and kept at 37°C in aerobic conditions for 12 days. Cell titer was measured once a day by serial dilution of the culture in LB medium and agar plating. To analyze cell sensitivity to heat stress, WT and I48S strains were transiently exposed to 45°C, and cell titer was measured by serial dilution of the culture in LB medium and plating aliquots of diluted culture on LB agar. For each strain, the drop in titers was calculated relative to non-stressed cells. To determine the percentage of dormant cells resistant to antibiotics, the wild-type and I48S strains were grown for 48 hours in MOPS minimal medium supplemented with glucose (0.2%) at 37°C followed by simultaneous addition of glucose (0.2%) and ampicillin (50 μg/ml) or ciprofloxacin (10 μg/ml). The cultures were incubated at 37°C and cell titer was measured at various time points.

De novo protein synthesis

Cells were grown for 48 h at 37°C in MOPS minimal medium (pH 7.2) supplemented with 0.2% glucose and a mixture of 19 amino acids (20 mg/l each) without valine. After 48 h of growth, the culture was supplemented with 0.1 μCi of L-[^{14}C]-valine (Perkin Elmer, USA) and grown for additional 2 h, thus allowing us to measure the intensity of protein synthesis in the stationary phase. Translation activity in the lag phase was measured by simultaneous addition of 0.1% glucose and 0.1 μCi of L-[^{14}C]-valine followed by 10 min of growth. For estimation of the L-[^{14}C]-valine incorporation efficiency in the exponential phase, the cells were supplemented with 0.1% of glucose and allowed to regrow for 2 h followed by addition of 0.1 μCi of L-[^{14}C]-valine and 10 min of incubation at 37°C. Incorporation of the radioactive amino acid was halted by centrifugation and two subsequent washes with PBS. The cell pellet was resuspended in 1× Laemmli Sample Buffer and incubated at 95°C for 5 min. Cell debris was removed by centrifugation and samples with equal amount of total protein were analysed by SDS-PAGE followed by autoradiography. Coomassie staining was used to control the total protein load.

Western blotting

Bacterial cultures were collected at different time points for preparation of total protein samples. The proteins were separated by SDS-PAGE (8%, 45 min, 220 V). Semidry transfer was performed for 90 min at 20 V using Amersham Protran 0.45 NC Nitrocellulose. Blocked membrane was incubated with primary monoclonal antibodies (Neoclone, 2G10 for σ^{70} and 8RBR for β subunit, 1:1000, 16 h, +4°C, 1% milk PBST). Secondary HRP-conjugated anti-mouse antibodies were used (1:5000, room temperature, 2 h, 1% milk PBST), and the bands were developed using the Luminata crescendo substrate (Millipore) in the chemiluminescence mode in ChemiDoc MP (Bio-Rad).

Flow cytometry analysis

To determine *in vivo* protein synthesis efficiency, the cells of the wild-type and I48S strains were transformed by a plasmid encoding the FastFT protein (28) under the control of the T5 promoter. Cells were grown in LB medium at 37°C for 24 hours followed by dilution with fresh LB medium. An aliquot was taken at indicated time points; cells were isolated by centrifugation, washed two times with sterile PBS and analyzed by fluorescence-activated cell sorter FacsAria III (Becton Dickinson and Company). Cells were detected using 488 nm laser side scattering (SSC) at cutoff value 1000. The blue form of the FastFT protein was quantified using 405 nm laser and 450/20 nm filter. The red form of the FastFT protein was quantified using 561 nm laser and 610/10 nm filter.

Genome sequencing and assembly

The genomes of BW25113 (the parent strain for the Keio Collection) and JW0836 (Keio *ΔrimK*) strains were sequenced using Illumina HiSeq2500 technology. Sequencing of NEBNext libraries generated 2,913,362 (JW0836) and 2,611,204 (BW25113) single-end reads (230 nt). Sequencing primers were removed using Cutadapt (29) and low quality read regions were trimmed using Sickle (https://github.com/najoshi/sickle). Illumina reads were assembled using SPAdes 3.7.1 (30). Contigs shorter than 200 bp were discarded.

Transcriptome analysis

Cells of the wild-type and I48S strains were grown at 37°C for 24 h followed by dilution with fresh LB medium. Cells were collected in the exponential phase ($OD_{600} = 0.6$) and in the stationary phase (48 h after dilution of cells with fresh LB). Total RNA was isolated using the TRIzol reagent according to the manufacturer's instructions (Thermo Scientific). The samples were treated with DNase I (Thermo Scientific) followed by purification using PureLink RNA Mini Kit (Thermo Scientific). RNA integrity for each sample was confirmed by denaturing PAGE. The level of rRNA was estimated by analysis of SYBR™-stained RNA gels with Fiji (modification of ImageJ) software (31).

mRNA library preparation was performed using the NEBNext® mRNA Library Prep Reagent Set for Illumina® according to the manufacturer's instructions

(New England Bio-Labs Inc., Ipswich, MA, USA). The libraries were sequenced using the Illumina HiSeq 2500 platform. At least 4.5 million of 50-bp single end reads were generated for each sample. We used previously assembled *E. coli* str. K12 substr. MG1655 (assembly GCA_000005845.2) as a reference for reads mapping. We used RSEM v1.3.1 to calculate gene expression levels for each sample and to perform statistical tests for differentially expressed genes.

RT-qPCR

Total RNA was isolated with TRIzol reagent (Invitrogen) according to the manufacturer's instructions. RNA integrity for each sample was confirmed by denaturing PAGE. One microgram of total RNA was treated with 1U of DNase I (Thermo Fischer Scientific) for one hour at 37°C and the reaction was stopped by addition of EDTA to 5 mM. cDNA was synthesized from total RNA using Maxima First Strand cDNA Synthesis Kit for RT-qPCR with a random hexamer primer (Thermo Fischer Scientific). Briefly, one microgram of DNase I-treated RNA was incubated with or without reverse transcriptase in 10 μl of the reverse transcription buffer for 10 min at 25°C followed by 30 min at 60°C. The samples were heated at 85°C for 5 min to inactivate reverse transcriptase. 2 μl of the 10-fold diluted cDNA or control RNA without reverse transcription were added per 15 μl of the qPCR reaction mixture. Quantitative PCR was performed under following conditions: 95°C for 5 min; 35 cycles at 95°C for 30 s, 54°C for 30 s, and 72°C for 1 min; 72°C for 10 min, then maintained at 4°C. The reactions were performed with SYBR™ Green PCR Master Mix (Thermo Fischer Scientific) in the CFX96 Touch™ Real-Time PCR Detection System and analysed by CFX Maestro Software (Bio-Rad). CT values were averaged, and the RNA expression level was calculated by the $2^{-\Delta\Delta CT}$ method and normalized to the expression level of 16S RNA. The primers were used at the final concentration of 500 nM and their sequences are shown in Supplementary Table S1.

Luciferase assay

Analysis of the *in vivo rrnB* P1 activity was performed as described in (32). WT or I48S *E. coli* strains were transformed with plasmid pET28_rrnBP1_luxCDABE encoding the complete luciferase operon from *Photorhabdus luminescence* under the control of the *rrnB* P1 promoter. The cells from overnight culture were diluted 20 times and grown in the presence of kanamycin (50 μg/ml) and chloramphenicol (20 μg/ml) in 1 l flasks in 75 ml LB at 30°C, 230 rpm. Luminescence measurements were performed after indicated time intervals in 100 μl samples in black plates in the Modulus luminometer (Turner BioSystems, USA). Optical density (OD_{600}) measurements were performed in parallel. Normalized luminescence values were obtained by dividing the raw luminescence data by the OD_{600} value in each sample.

Protein purification

Escherichia coli core RNAP was expressed from the pVS10 plasmid and purified as described previously (33). Wild-type σ^{70} containing an N-terminal His_6-tag was expressed from the pET28-*rpoD* vector and purified from inclusion bodies, followed by protein renaturation and Ni-affinity chromatography (3,32). Mutant σ^{70} containing the I48S substitution was obtained by site-directed mutagenesis and purified in the same way. DksA containing an N-terminal His_6-tag was expressed in *E. coli* BL21(DE3) from the pET28-DksA plasmid (32). All buffer solutions used during DksA purification contained 0.1 mM $ZnCl_2$. After cell lysis, RNAP and associated proteins were removed by Polymin P precipitation (33), proteins from the unbound fraction were precipitated with ammonium sulfate and separated using Ni-NTA-affinity chromatography. DksA was dialyzed against storage buffer, supplemented with glycerol (final buffer composition, 40 mM Tris–HCl, pH 7.9, 55 mM NaCl, 0.55 mM EDTA, 1 mM DTT, 0.1 mM $ZnCl_2$, 50% glycerol) and stored at −70°C.

CD measurements

CD spectra of wild type σ^{70} and I48S mutant were measured using a Chirascan CD spectrometer (Applied Photophysics, UK). Proteins were purified as described in 'Protein purification' section. Experiments were performed at 25°C in a quartz glass cell with a 0.1 mm path length. Spectra (190–260 nm) were recorded with a total of five scans for each sample. The molar ellipticity was calculated based on the concentration verified by Qubit™ Protein Assay Kit (Invitrogen).

In vitro transcription

Supercoiled pTZ19-based plasmid containing the RNA I promoter (108–110 nt full-length RNA) and *rrnB* P1 promoter followed by the *hisT* terminator (88 nt full-length RNA) was obtained as described in (32). Linear DNA fragments containing the *rrnB* P1, T7A1cons or λP_R promoters (Supplementary Figure S5) were obtained by PCR from synthetic oligonucleotides and plasmid templates (3). For measurements of RNAP activity on the plasmid DNA template, core RNAP (50 nM final concentration in most experiments) was mixed with wild-type or I48S σ^{70} subunits (250 nM in most experiments) in reaction buffer containing 40 mM Tris–HCl, pH 7.9, 10 mM $MgCl_2$ and 150 mM KCl (for experiments in Figure 6C, D) or 40 mM KCl (for other experiments). Supercoiled plasmid (10 nM) was added and the samples were incubated for 5 min at 37°C, followed by the addition of DksA (2 μM), ppGpp (200 μM, TriLink Biotechnologies), or 6S RNA, when indicated. After 5 min, NTP substrates were added at the following final concentrations: 200 μM ATP, CTP, GTP; 10 μM UTP (with α-[^{32}P]-UTP), and 25 μM CpA primer (in most assays except for the ATP K_M measurements). Analysis of RNAP activity on the T7A1cons and λP_R templates was performed in a similar way; for λP_R, 25 μM ATP, GTP, ApU and 0.5 μM UTP (with α-[^{32}P]-UTP) was added for 26-mer RNA synthesis; for T7A1cons, 25 μM ATP, CTP, GTP, 0.5 μM UTP (with α-[^{32}P]-UTP) and 10 μg/ml heparin was added for 53 nt run-off RNA synthesis. For analysis of the efficiency of promoter escape on the T7A1cons template, 10 μM ATP, CTP, GTP, 5 μM UTP (with α-[^{32}P]-UTP) and 25 μM CpA was added. Transcription was performed for 5–10 min at 37°C

and stopped with an equal volume of solution containing 8 M urea and 20 mM EDTA. RNA products were separated by 15% or 20% urea–PAGE and analyzed by phosphorimaging.

To measure promoter complex stability on *rrnB* P1, promoter complexes were obtained in transcription buffer containing 40 mM Tris–HCl, pH 7.9, 10 mM $MgCl_2$ and 40 mM KCl. Heparin (10 μg/ml) or a fork-junction competitor DNA (2 μM) containing the –10 element and a short downstream duplex (upper DNA strand, 5′-TATAATGG GAGCTGTCACGGATGCAGG; bottom DNA strand, 5′-CCTGCATCCGTGAGTGCAG; the -10 element is underlined) was added for indicated time intervals before NTP addition. In the experiments with the heparin competitor, 200 μM ATP, CTP, GTP and 5 μM UTP (with α-[^{32}P]-UTP) were added together with heparin (10 μg/ml); in the case of the fork-junction competitor, 25 μM CpA, 200 μM ATP, CTP, GTP and 10 μM UTP were added together with rifapentin (5 μg/ml). The presence of heparin or rifapentin in the nucleotide mixtures was required to prevent transcription re-initiation in control reactions lacking DNA competitors. The data were fitted to a one-exponential equation to determine the observed rate constants (k_{obs}) and half-life times ($t_{1/2} = \ln 2/k_{obs}$) for dissociation of promoter complexes (32).

To measure apparent affinities of DksA, promoter complexes were incubated with increasing concentrations of DksA (from 10 nM to 30 μM) in the absence or in the presence of ppGpp (200 μM), followed by the addition of NTP substrates, and the data were fitted using the hyperbolic equation: $A = A_{max} \times (1 - [DksA]/(K_{d,app} + [DksA]))$, where A_{max} is RNAP activity in the absence of DksA and A is RNAP activity at a given DksA concentration.

UV crosslinking

Ultraviolet light-induced σ-DNA crosslinking was performed as described in (34). Wild-type or I48S σ subunits were incubated at various concentrations with a 5′-labeled ssDNA oligonucleotide containing the –10 promoter element (100 nM; see Figure 6A) in 10 μl of the transcription buffer for 10 min at 37°C. The samples were transferred to 25°C and irradiated for 5 minutes at 254 nm with a 4 W UV lamp (Spectroline) placed on the top of open 1.5 ml tubes. The samples were analysed by 8% denaturing PAGE and phosphorimaging.

DNA footprinting

$KMnO_4$ and Exonuclease III (Exo III) footprinting experiments were performed with linear DNA containing the *rrnB* P1 promoter (positions –72 to +38); nontemplate or template promoter strands were labeled during PCR with 5′-^{32}P-primers. $KMnO_4$ footprinting was performed as in (35). Promoter complexes (100 nM core RNAP, 500 nM σ^{70}, 20 nM promoter DNA) were obtained in reaction buffer containing 40 mM Tris–HCl pH 7.9, 10 mM $MgCl_2$ and 40 mM KCl for 15 min at 37°C; DksA (2 μM) was added when indicated. ATP and CTP were added (200 μM) for 1 min, and the samples were treated with 2 mM $KMnO_4$ for 30 s, followed by the addition of a stop-solution containing 1 M β-mercaptoethanol and 1 M sodium acetate (pH 4.8). DNA was precipitated with three volumes of ethanol, treated with 10% piperidine for 15 min at 95°C, treated with water-free chloroform, ethanol-precipitated, dissolved in urea-containing loading buffer, and analyzed by 15% PAGE.

Exo III footprinting was performed as in (36). Promoter complexes were obtained in the reaction buffer with 50 nM core RNAP, 250 nM σ^{70} and 10 nM promoter DNA. NTP substrates were added to a subset of reactions (50 μM CpA, 100 μM CTP, UTP, GTP) to allow synthesis of up to 5 nt long RNA products, 30 seconds before ExoIII addition. The samples were incubated with 5 units of Exo III (New England BioLabs) at 37°C, followed by the addition of a formamide stop-solution, and analyzed by 10% denaturing PAGE. The A+G cleavage marker was obtained by treatment of the promoter DNA fragment with formic acid and piperidine.

RESULTS

ΔrimK strain from the Keio collection harbors a point mutation in the *rpoD* gene that explains its unusual phenotype

Ribosomes of all living organisms are subjected to numerous post-transcriptional and post-translational modifications. One of the most unusual modifications of bacterial ribosomal proteins is the post-translational addition of glutamic acid residues to the C-terminal end of ribosomal protein S6 (37). This modification is performed by the RimK L-glutamate ligase. While studying possible cellular functions of this modification, we found that the *ΔrimK* strain from the Keio collection (38) has multiple phenotype abnormalities related to survival and metabolic activity of bacterial cells. A particular feature of this strain was a decreased titer of dormant cells, which are known to possess extreme resistance to antibiotics thus making this strain especially interesting to research.

Unexpectedly, experiments with complementation of *rimK* gene expression from a plasmid vector failed to restore the wild-type phenotype, despite the fact that modification of S6 was present in that type of cells. Moreover, P1 transduction of the *ΔrimK* locus from the Keio strain to the wild-type strain and independent knockout of the *rimK* gene demonstrated minor influence of *rimK* on cell fitness (39). Considering the results of these experiments, we proposed that phenotype abnormalities of the Keio *ΔrimK* strain might be caused by an additional mutation.

Consistent with our assumption, whole genome sequencing of the Keio *ΔrimK* and wild-type strains revealed that the former possesses a point mutation T143G in the coding region of the *rpoD* gene that results in a substitution of isoleucine to serine (I48S) in region 1.1 of the RNA polymerase σ^{70} factor. In order to study the impact of the I48S mutation on bacterial cell fitness we utilized the lambda RED system to construct a BW25113-based strain with the T143G substitution in the *rpoD* gene as well as a control strain without mutation. As described in the following sections, the I48S strain revealed the same growth abnormalities as the *ΔrimK* strain from the Keio collection thus confirming that the *rpoD* mutation is responsible for the unusual phenotype of the original strain.

The I48S mutation results in delayed growth resumption from stationary phase and makes the cells more susceptible to antibiotics

To check whether the mutation might affect σ^{70} levels in the cell we performed Western blotting analysis of protein extracts isolated from the wild-type or mutant strains. The analysis revealed no differences in the amounts of σ^{70} in these strains at different stages of growth (Supplementary Figure S1). Furthermore, since substitution D61A is known to cause σ^{70} thermolability (12), we measured colony forming units (CFU) for the I48S strain after transient exposure to 45°C and found that this number was the same as in the wild-type strain (the drop in cell titer was 353 ± 89-fold and 268 ± 123-fold for WT and I48S strains, respectively). This suggested that the mutation does not affect σ^{70} expression and/or stability.

To understand the possible impact of the I48S substitution on bacterial cells fitness, we compared the growth rates of the wild-type and I48S strains. The doubling time in the exponential phase was comparable for the WT and I48S strains (40.8 ± 1.7 min and 46.4 ± 2.1 min in LB medium, 142.6 ± 12.8 min and 176.4 ± 4.8 min in MOPS minimal medium, 125.9 ± 6.1 min and 146.1 ± 5.3 min in minimal medium with 20 amino acids, respectively). However, the I48S strain exhibited a significant delay during transition to the exponential phase. The average lag phase duration for the WT and I48S strains was 56.3 ± 2.7 min and 95.3 ± 1.7 min in LB medium (Figure 2A), 258.4 ± 9.4 min and 321.6 ± 12.1 min in MOPS minimal medium, and 119.8 ± 6.1 min and 211.6 ± 5.7 min in minimal medium with 20 amino acids (Figure 2B).

To check whether the phenotypic difference between the wild-type and mutant cells might be connected to changes in cell appearance, we visualized the cells by fluorescent microscopy combined with simultaneous DNA and membrane labelling by DAPI and FM^{TM} 4–64 fluorophores (Supplementary Figure S2). We found no differences in the cell size or morphology at different growth phases between the WT and I48S cells.

One possible reason for the observed extended lag phase could be a lower titer of cells capable of regrowth after the stationary phase. However, we found that the CFU numbers were similar for the wild-type and I48S strains at different times of incubation at the stationary phase conditions (from 1 to 12 days) suggesting that cell survival and the ability to regrowth is not affected by the mutation (Figure 2C).

Another possible reason for the extended lag phase could be abnormal metabolic adaptation of the mutant strain during growth resumption from stationary phase. One of the strategies contributing to bacterial cells survival is formation of various dormant forms (40), which have reduced metabolism and possess extreme insensitivity to antibiotics (41). Upon transition to conditions favorable for fast growth of bacterial population, they split into actively growing and dormant subpopulations (42). Dormant bacteria are characterized by metabolic quiescence, including inhibition of protein synthesis (43). Sudden exposure to antibiotics devastates actively growing cohorts while preserving dormant forms intact (42).

To test possible effects of the I48S mutation on the formation of dormant cells, we transiently exposed bacterial cultures in the lag phase to ampicillin, which is known to possess bactericidal effect on metabolically active cells so that only dormant cells could survive transient ampicillin treatment. After washing out ampicillin the cells were plated on agar and the titer of survived cells was determined. Unexpectedly, it was found that the titer of dormant cells in the I48S strain was significantly lower than that in the control strain during the first three hours of incubation with ampicillin (Figure 2D). This suggested that a higher proportion of cells in the mutant strain culture immediately activated their metabolism after addition of fresh nutrients to the stationary culture, while 'awakening' of the wild-type strain was delayed, thus making it less susceptible to antibiotic treatment. Indeed, prolonged incubation with ampicillin led to a similar drop in cell titer for both strains (Figure 2D). Similar results were obtained after incubation of the wild-type and I48S cells with ciprofloxacin, demonstrating that the mutation makes bacteria more susceptible to antibiotics from different classes (Figure 2E).

The I48S mutation changes the dynamics of protein synthesis during culture growth

To further reveal the effects of the I48S mutation on cell metabolism we used pulse labeling of newly synthesized proteins with L-[^{14}C]-valine, which allows to evaluate total protein synthesis intensity in the cells at a given phase of growth. Although the total protein synthesis efficiency in the exponential phase was comparable for the wild-type and I48S strains, the protein synthesis profile differed dramatically (Figure 2F, left). In the stationary phase wild-type cells efficiently ceased protein synthesis, while the I48S cells retained a much higher level of translation. In this case, the pattern of newly synthesized proteins in the mutant strain was more similar to the wild-type cells than in the exponential phase (Figure 2F, middle). Similarly, a higher level of protein synthesis in the mutant strain was observed during growth resumption from stationary phase (Figure 2F, right). These results suggest that the I48S cells might have a higher level of synthetic activity during regrowth.

To observe the dynamics of gene expression in individual cells in the population of bacteria throughout the growth cycle, we utilized a fluorescent protein timer, FastFT (28). The FastFT protein undergoes the first step of maturation with the half-reaction time of 0.25 h resulting in a protein with blue fluorescence. The next maturation step leads to a red fluorescent protein, with half-reaction time of 7.1 h, thus making it possible to investigate the dynamics of protein biosynthesis in the cell (Figure 3A).

The plasmid with the FastFT protein gene placed under the control of a σ^{70}-dependent T5 promoter was introduced to the wild-type and I48S strains. Both wild-type and I48S bacterial cultures were incubated for 48 hours to reach the stationary phase; during this period the FastFT protein that was synthesized in the exponential phase had sufficient time to maturate to its red form. The stationary phase cultures were analyzed by flow cytometry to determine the ratio of the FastFT blue form continuously synthesized in the sta-

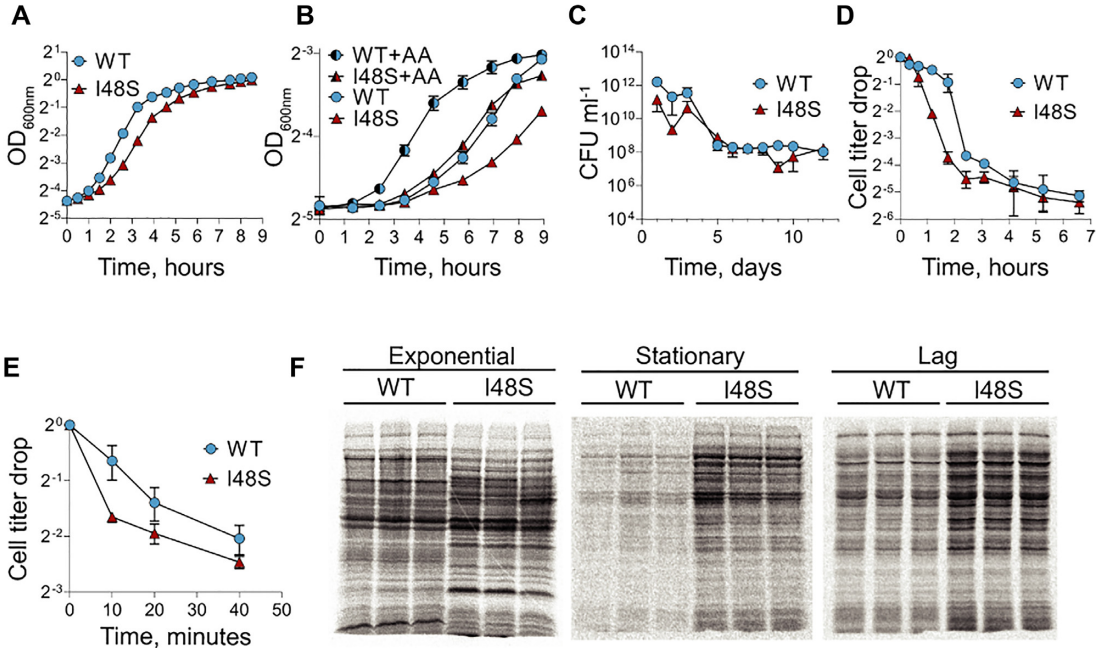

Figure 2. Analysis of the mutant strain fitness. (**A**) Growth curves ($\log_2$ scale) of the wild-type (blue) and I48S strains (carmine) in LB medium. Each point represents six independent replicates. (**B**) Growth curves ($\log_2$ scale) of the wild-type (blue) and I48S strains (carmine) in MOPS minimal medium in the absence and in the presence of 20 amino acid supplements. Each point represents three independent replicates. (**C**) Survival of the wild-type (blue) and I48S strains (carmine) in the stationary phase. Each point corresponds to a cell titer ($\log_{10}$ scale) of three independent replicates at indicated time of growth. (**D**) Ampicillin susceptibility test in MOPS minimal medium. Cells were grown for 48 hours and allowed to regrow by simultaneous addition of glucose (0.2%) and ampicillin (50 μg/ml). Cell titer was measured at the indicated time of growth with ampicillin. Cell titer drop was calculated as (cell titer at t_n)/(cell titer at t_0). Each point represents three independent replicates. (**E**) Ciprofloxacin susceptibility test in MOPS minimal medium. Cells were grown for 48 h and allowed to regrow by simultaneous addition of glucose (0.2%) and ciprofloxacin (10 μg/ml). Cell titer was measured at the indicated time of growth with ciprofloxacin. Cell titer drop was calculated as (cell titer at t_n)/(cell titer at t_0). Each point represents three independent replicates. (**F**) *De novo* protein synthesis at the indicated phase of growth in MOPS minimal medium supplemented with 0.2% glucose and a mixture of 19 amino acids with addition of L-[^{14}C]-valine (see Materials and Methods for details). Each lane represents a protein sample from independent replicate.

tionary phase and the FastFT red form made in the preceding exponential growth phase (scheme in Figure 3A). The results indicated that wild-type bacteria efficiently ceased protein synthesis in the stationary phase as expected (Figure 3B, panel (a), 4%), while the culture of the mutant cells contained a substantial population of cells with active synthesis of the blue form of the FastFT protein (Figure 3B, panel (b), 22%).

Moreover, dilution of the stationary phase cultures with fresh media differently affected the wild-type and I48S cells. One hour after transition to the fresh media wild-type cells formed three populations (Figure 3B, panel (c)). The majority of wild-type cells remained quiescent (49%), while 27% of culture were represented by already divided cells (the population with decreased red fluorescence) and 23% of cells synthesized the blue form of the FastFT protein without division (the population with increased blue fluorescence but without any reduction of the red fluorescence). In contrast, only 34% of I48S cells remained quiescent and four distinct populations were observed, with an additional population formed by divided cells with high synthetic activity (Figure 3B, panel (d), the lower population with increased blue fluorescence and decreased red fluorescence marked with an arrow). Upon 3 h of incubation in fresh media, 37% of wild-type cells remained quiescent (Figure 3B, panel (g)), in contrast to 10% of I48S cells (Figure 3B, panel (h)). Dynamics of FastFT synthesis in WT and I48S cells during transition to exponential phase demonstrated that the WT strain tended to save quiescent population even after 7 h of incubation in fresh media (Figure 3B, panels (i, k, m, o)), while no dormant cell population was apparent in the case of the I48S strain after 6 h of growth (Figure 3B, panels (j, l, n, p)). It should be noted that the share of dividing cells was almost unchanged for both strains at all time points after 2 h of incubation. The observed reduction of the quiescent cells population in the I48S strain is mostly explained by the presence of a higher number of non-dividing cells with an increased synthetic activity than in the case of the WT strain (Figure 3B, panels (c, d), the upper right quadrant).

Thus, upon dilution with fresh medium the population of wild-type cells from the stationary phase splits into actively growing and dormant cells. In contrast, the stationary phase I48S cells start to synthesize proteins instantly upon transition to fresh medium. These results correlate with the decreased number of dormant cells and increased level of protein synthesis in the mutant strain revealed in the previous experiments. Overall, these results suggest that the observed delay in the transition from stationary to exponential growth characteristic for the mutant strain could be explained by dysregulation of transcription and/or protein synthesis caused by the I48S mutation.

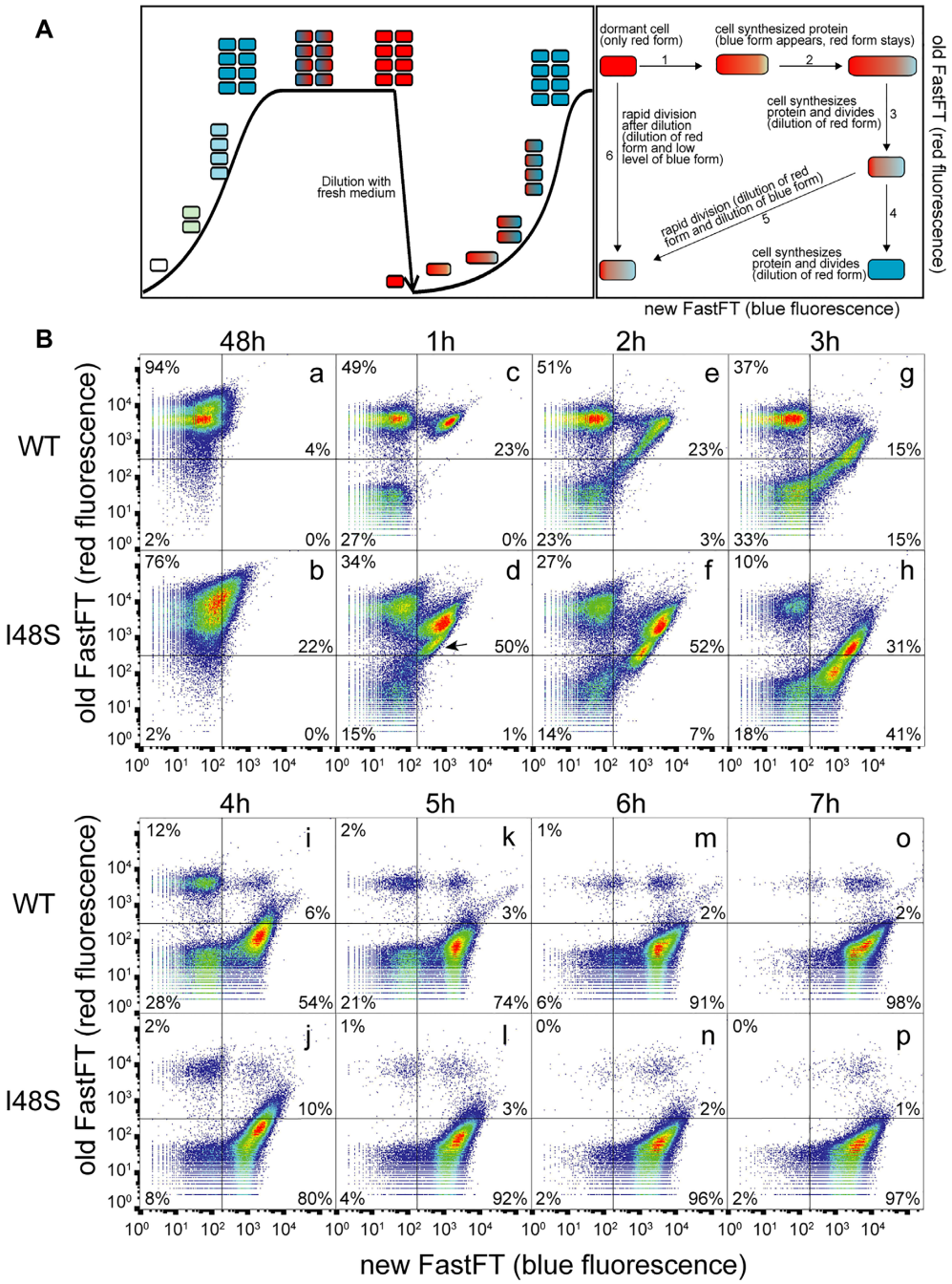

Figure 3. Synthesis of the FastFT fluorescent protein timer by the wild-type and I48S cell cultures upon exit from stationary phase. (**A**) Scheme of the experiment for monitoring the metabolic activity with fluorescent timer protein FastFT. (Left) Changes in the FastFT protein synthesis and maturation throughout the growth curve of bacterial culture. (Right) Subpopulations of cells with various levels of the red and blue forms of FastFT formed during transition from the stationary phase to the exponential phase of growth. (**B**) Scatter plots for bacteria analyzed by flow cytometry. The x- and y-axes correspond to the blue and red fluorescence intensity, respectively. Percent of cells in the indicated subpopulation in each quadrant is shown. Pseudocolors correspond to cell density. Panel (a) Scatter plot corresponding to the wild-type cells in the stationary phase. Panel (d) Scatter plot corresponding to the I48S cells in the stationary phase. Panels (c, e, g, i, k, m, o) scatter plots corresponding to the wild-type cells after 1, 2, 3, 4, 5, 6 and 7 h post dilution with the fresh LB medium. Panels (d, f, h, j, l, n, p) scatter plots corresponding to the I48S cells after 1, 2, 3, 4, 5, 6 and 7 h post dilution with the fresh LB medium.

Effects of the I48S mutation on the *E. coli* transcriptome

In order to study the transcriptional effects of the I48S mutation on the whole genome level, WT and I48S cells from exponential and stationary phases were collected at $OD_{600} = 0.6$ and after 48 h of growth, respectively, with subsequent total RNA isolation. Notably, the intensity of the 16S and 23S rRNA bands in denaturing gel was higher in the mutant strain in the exponential phase of growth, suggesting that the mutant cells have a higher level of rRNA expression or stability (Supplementary Figure S3). RNA samples from three biological replicates for each strain and growth phase were sequenced. RNA-seq analysis revealed that the rRNA level in the I48S strain was 85–87% of total RNA compared to 73–78% of total RNA for the wild-type strain, consistent with the results of the PAGE analysis. Additionally, a differential expression analysis was performed for protein-coding genes. Initial analysis was performed by the 'Functional annotation' tool on the David webserver (44) and 'Analysis' tool on the STRING database webserver (45). Significantly affected pathways were then identified with the help of KEGG and GO. It was found that the expression levels of 886 and 148 genes were significantly altered in exponential and stationary phases, respectively ($|FC| \geq 1.5$; adjusted PPEE value < 0.05) (Figure 4A, Supplement files 1 and 2). The changes in the expression levels of certain genes (randomly selected genes responsible for growth promotion, stress response and metabolic activity) were further verified by RT-qPCR (Supplementary Figure S4). For all analyzed genes (10 for each growth phase), the results were in a good agreement with the RNA-seq analysis.

Differentially expressed genes in the exponential phase are enriched for multiple pathways. The functional categories of upregulated genes in the I48S strain include flagellar assembly (37 genes), bacterial chemotaxis (17 genes), ribosome (40 genes, rRNA and ribosomal proteins), ribosome biogenesis (15 genes, ribosome assembly and maturation factors), translation (14 genes, translation factors and aminoacyl-tRNA synthetases), biosynthesis of amino acids (27 genes) and fatty acid biosynthesis (9 genes), whereas downregulated genes are enriched with transcription regulation (62 genes), stress response (26 genes) and various carbon (18 genes) and lipopolysaccharide (7 genes) metabolism pathways. In order to understand regulatory pathways affected by the I48S mutation, we visualized our RNA-seq data with the help of the 'Omics Dashboard' tool on the EcoCyc webserver (46). Transcriptome analysis by 'Omics Dashboard' revealed complex dysregulation of the σ factors network (Figure 4B). Consistent with gene enrichment analysis, the activity of the σ^{28} regulon, responsible for flagellar biosynthesis, was significantly increased. In contrast, the activity of the σ^{38} regulon was decreased, with downregulation of genes responsible for cellular stress response. The apparently increased activity of the σ^{32} could be mostly attributed to upregulation of rRNA genes, which are controlled by both σ^{70} and σ^{32}. In summary, sigmulon activity analysis showed a distinct shift of gene expression from stress-related to growth-promoting processes, such as ribosome biosynthesis and locomotion. It should be noted that the observed changes in the expression of genes encoding for master regulators of transcription and σ factors (Figure 4C) make it hard to distinguish between the primary and secondary transcriptional effects of the I48S mutation.

Strikingly, all of the enriched pathways among upregulated differentially expressed genes in the exponential phase in the mutant strain have been described to be regulated by DksA and the stringent response (47). We also noted some similarities in gene expression between the I48S strain and previously studied Δ*dksA* strains. In particular, promoter activity of genes encoding rRNA (*rrnB* P1), ribosomal proteins (*rpsNp*, *rpsU* P2 and others), flagellar cascade components (*flhDp* and *fliAp1*) and fatty acid biosynthesis pathway (*fabHp*) is also significantly increased in Δ*dksA* strains, even in the exponential phase of growth (48–51). Microarray study of Δ*dksA E. coli* strain (52) revealed a strong upregulation of genes involved in flagellar assembly and chemotaxis and downregulation of stress response genes, similarly to I48S. In contrast, DksA is essential for activation of genes responsible for biosynthesis of amino acids, yet this pathway is significantly enriched in the upregulated genes of the I48S strain (53). At the same time, the I48S mutation did not significantly affect the expression of genes involved in the regulation of the stringent response itself, with unchanged levels of *relA* (encoding for the ppGpp synthase RelA) and slightly upregulated expression of *spoT and dksA* (Supplement file 1 and 2).

Among the functional categories of upregulated genes in the stationary phase are metabolic pathways (9 genes), while downregulated genes are enriched with transcription regulation (19 genes) and stress response pathways (8 genes). It should be noted that 45% of differentially expressed genes encode putative proteins with unknown function, which may reflect poor understanding of the stationary phase-specific pathways, since most of previous *E. coli* studies were conducted on cells in the exponential phase of growth. Downregulated genes of particular interest are *raiA*, *rmf* and *sra. raiA* and *rmf* encode for hibernation factors of ribosome responsible for translation inhibition at the onset of stationary phase (54). Although the function of Sra (also known as the S22 protein) is not fully understood, it was shown to be associated with ribosomes in the stationary phase of growth (55). Finally, we revealed changes in the expression of 6S RNA, which suppresses the activity of the σ^{70} RNAP holoenzyme during the stationary phase (56,57), using the RNA-seq data and RT-qPCR. It was found that the expression level of 6S RNA, encoded by the *ssrS* gene, was decreased 1.5–2-fold in the stationary culture of the mutant strain (Supplementary Figure S4C). Similarly, the expression of 6S RNA was higher in wild-type cells than in the mutant in the exponential phase. Downregulation of genes required for translation and transcription repression may partially explain the phenotype of increased protein synthesis rate and, consequently, decreased number of dormant cells in the stationary phase.

Possible effects of the I48S substitution on σ^{70} conformation

Previously, deletions in region 1.1 were shown to increase the ability of free σ^{70} to interact with DNA, likely because region 1.1 masks the DNA binding sites in re-

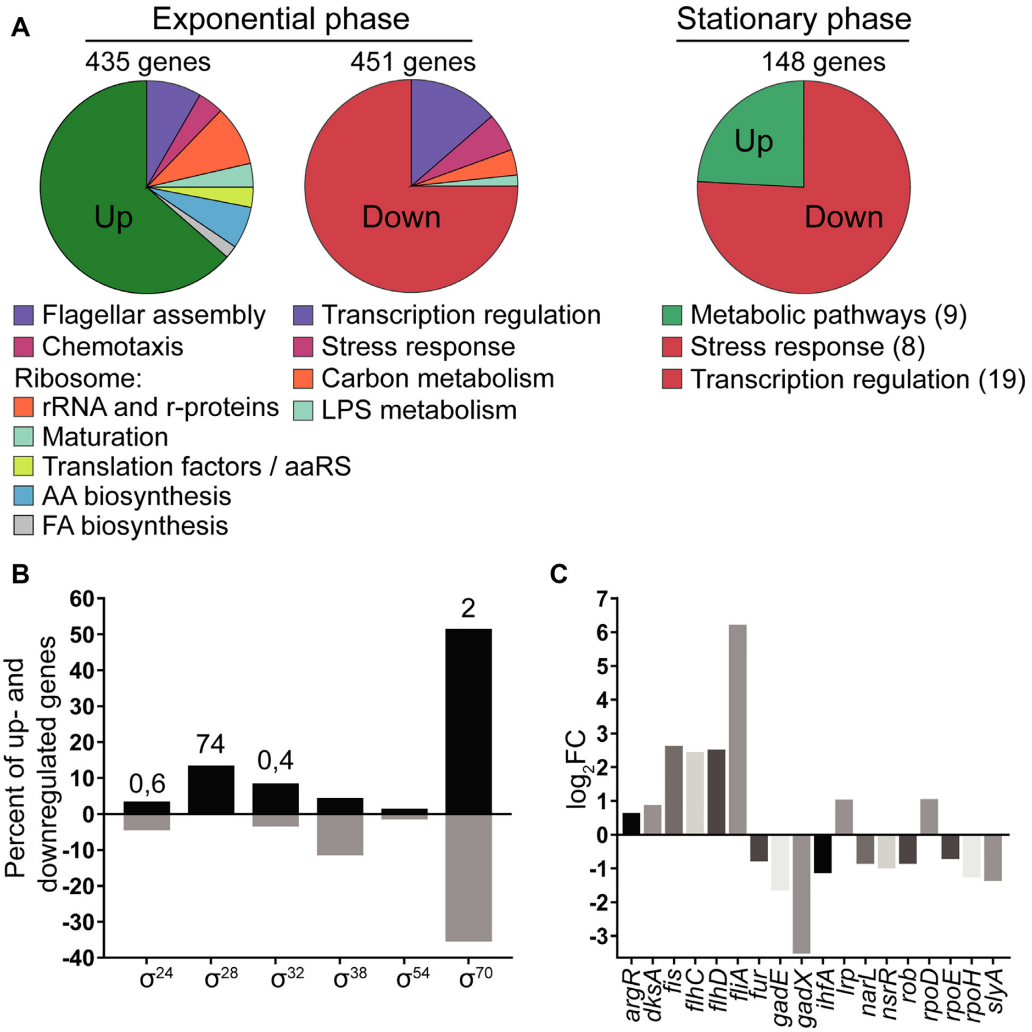

Figure 4. Transcriptome analysis of the mutant strain. (**A**) Pie charts representing a number of downregulated and upregulated genes (Fold-Change |FC| ≥ 1.5; adjusted PPEE value < 0.05) in exponential and stationary phases of the mutant strain culture. Enriched pathways are shown below the corresponding pie chart. (**B**) Column graph representing percent of downregulated and upregulated genes in the exponential phase corresponding to different σ factor regulons. FC in the expression of genes encoding corresponding σ factors are shown above columns. (**C**) Column graph of differentially expressed master regulators of transcription and σ factors in the exponential phase.

gions 2 and 4 (13,14,58). To test whether the I48S substitution might affect the DNA binding properties of the σ factor, we analyzed the interactions of free σ^{70} with a single-stranded oligonucleotide containing the –10 promoter motif (TATAAT). Previous studies demonstrated that such interactions can be used to probe the conformational changes in σ^{70} required for unmasking of its DNA binding sites (34,58,59). The mutation significantly stimulated UV-induced protein-DNA cross-linking, especially at high σ concentrations (Figure 5A). The result suggests that the I48S substitution may affect the conformation of σ^{70} resulting in the exposure of its DNA binding regions. Indeed, comparison of circular dichroism (CD) spectra for the WT and I48S σ variants reveals small but detectable changes in the CD signal between 195 and 220 nm, suggesting that the mutation induces structural changes in σ^{70}, although the precise interpretation of these changes is difficult (Figure 5B).

Effects of the I48S substitution on the rRNA promoter activity and its regulation by DksA/ppGpp

To understand the impact of the I48S substitution on the activity of RNAP holoenzyme and its interactions with promoters, we performed a series of *in vitro* tests with the wild-type and I48S RNAPs. In particular, since the mutation affected rRNA expression and translation regulatory pathways *in vivo*, we focused on the *rrnB* P1 promoter that controls the expression of one of the seven rRNA operons in *E. coli* and is one of the best characterized cellular promoters (Figure 6A) (60,61). The activity of *rrnB* P1 is exceptionally high during exponential cell growth but is suppressed during the stationary phase. In contrast to most model promoters, the complexes of *E. coli* RNAP with *rrnB* P1 are highly unstable, which facilitates promoter escape but makes the promoter highly sensitive to regulatory factors. In particular, the activity of *rrnB* P1 is inhibited at the stationary phase or during stringent response by the transcription fac-

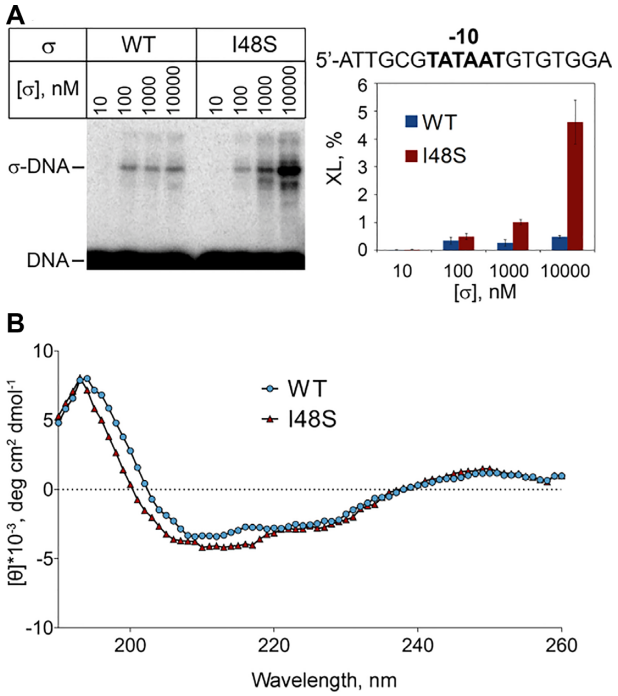

Figure 5. Effects of the I48S substitution on the conformation of σ^{70} and its interactions with DNA *in vitro*. (**A**) Analysis of σ-DNA interactions by UV-induced cross-linking. The ssDNA oligonucleotide containing a –10-like motif corresponding to the nontemplate promoter strand (shown on the top right) was incubated with increasing amounts of free σ^{70}, either wild-type or I48S, irradiated at 254 nm, and the complexes were separated by SDS-PAGE. Quantification of the crosslinking efficiencies (in percent of the total DNA in the sample) is shown on the right (means and standard deviations from three independent experiments). (**B**) Analysis of changes in the σ^{70} conformation by CD measurements. The spectra (190–260 nm) were recorded with a total of five scans for each sample.

tor DksA (stably expressed in the cell) and small alarmone ppGpp (synthesized upon stress conditions and starvation) that act synergistically (32,48,60,62,63). DksA destabilizes promoter complexes by binding within the secondary channel of RNAP, while ppGpp enhances its action through binding at the DksA–RNAP interface (ppGpp site 2) and between the β′ and ω subunits (site 1) (49,62–66). Both factors were proposed to affect promoter complex stability and interfere with promoter DNA melting, in particular, through changes in RNAP contacts with the downstream DNA duplex (62–65).

To confirm that the activity of the *rrnB* P1 promoter *in vivo* is affected by the I48S mutation, we used a reporter plasmid in which the luciferase operon from *Photorhabdus luminescens* (luxCDABE) was put under control of *rrnB* P1. It was found that the growth defects of the I48S strain were exacerbated in the presence of the *rrnB* P1 plasmid (Figure 6B, left) (with comparable plasmid content in both strains, ∼6/7 and 8/9 μg per 1 OD for the WT/I48S strains in exponential and stationary cultures, respectively), suggesting that the growth defect is caused by further dysregulation of gene expression in the presence of multiple copies of plasmidic *rrnB* P1. In the wild-type strain, the activity of the *rrnB* P1 promoter was high at the exponential phase of growth and was dramatically decreased at the stationary phase. Normalized activity values (lux/OD) of luciferase expressed from the *rrnB* P1 promoter were greatly increased (∼5-fold) for the I48S mutant strain at all OD values (Figure 6B, middle and right), confirming that the I48S mutation increases rRNA transcription *in vivo*.

We next performed *in vitro* analysis of the *rrnB* P1 activities with the wild-type and I48S RNAP variants using a supercoiled plasmid template containing the *rrnB* P1 promoter followed by the *hisT* terminator, resulting in synthesis of an 88 nt terminated RNA product (Figure 6C). The plasmid also contained an RNA I promoter in the RNAP-dependent pMB1 origin of replication, resulting in synthesis of the RNA I transcript of 108–110 nt. Previous studies demonstrated that, in contrast to *rrnB* P1, RNA I promoter forms highly stable complexes with RNAP, and transcription of RNA I is resistant to the action of DksA and ppGpp (32,49,62). The ratio of activities of these two promoters was therefore used as a measure of *rrnB* P1 regulation.

In the absence of any regulatory factors, the I48S RNAP holoenzyme had a higher activity on *rrnB* P1 relative to the RNA I promoter compared to wild-type RNAP (∼1.5-fold difference; Figure 6C and D). DksA (2 μM) slightly decreased the activity of WT RNAP on *rrnB* P1 but had no significant effect on the I48S mutant at this concentration. ppGpp (200 μM) similarly acted on wild-type RNAP and also decreased the activity of the mutant. When added together, DksA and ppGpp suppressed the activity of both RNAPs ∼2.0–2.5-fold. Notably, however, the activity of the mutant RNAP remained higher even in the presence of both factors (∼2-fold, Figure 6C and D). Thus, the I48S mutation results in an increased *rrnB* P1 activity both *in vivo* and *in vitro*, both in the absence and in the presence of DksA and ppGpp. In contrast, the activities of both WT and I48S RNAPs were not affected by DksA in the case of the RNA I promoter (Figure 6C) and of two strong bacteriophage-derived promoters, T7A1cons and λP_R (Supplementary Figure S5A and S5B), that form stable complexes with RNAP.

To investigate the reasons for the increased resistance of the I48S RNAP to DksA, we compared the activities of the wild-type and mutant RNAPs at different DksA concentrations. It was shown that the I48S mutant required higher concentrations of DksA to achieve the same level of inhibition (IC_{50} of 920 ± 340 versus 5100 ± 1800 nM for WT and mutant RNAPs, respectively) (Figure 6E, top). Similarly, the mutant RNAP was less efficiently inhibited by DksA when transcription was performed in the presence of ppGpp (IC_{50} of 650 ± 120 versus 2150±620 nM). At the same time, the maximal levels of inhibition at saturating DksA concentrations were comparable for both RNAPs (Figure 6E), suggesting that the mutation likely decreases DksA affinity to RNAP.

Effects of the I48S substitution on RNAP–promoter interactions *in vitro*

The enhanced activity of the mutant RNAP on the *rrnB* P1 promoter, observed in the absence as well as in the presence of DksA and ppGpp, could be explained by several factors, including changes in σ-core interactions, promoter

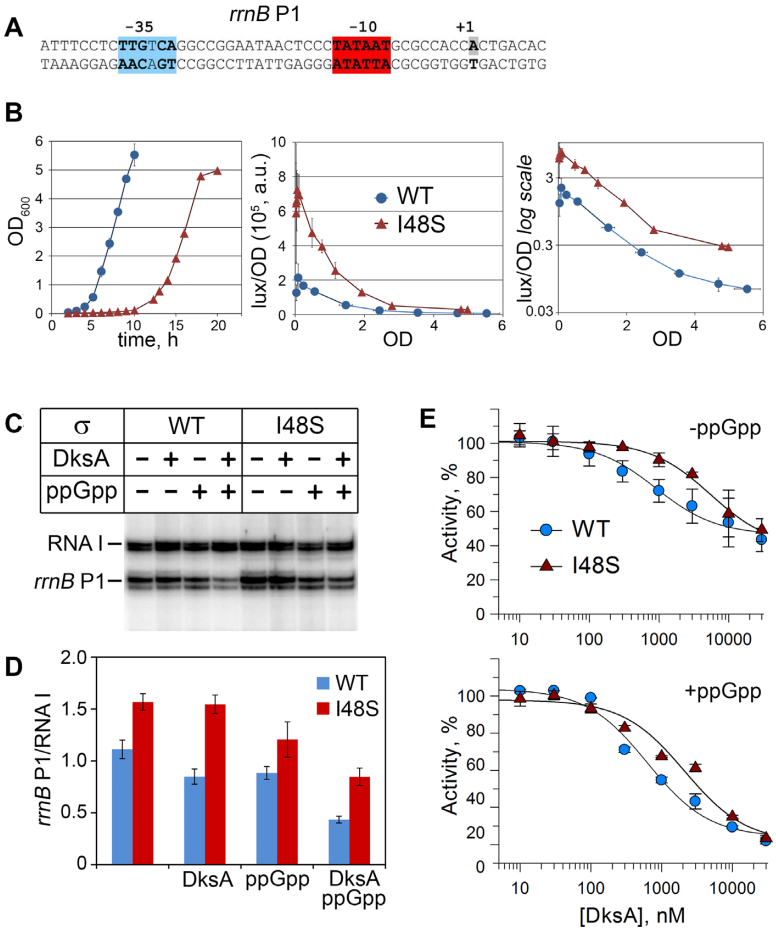

Figure 6. Effects of the I48S substitution on the activity of *rrnB* P1 promoter and its regulation by DksA and ppGpp. (**A**) Sequence of the *rrnB* P1 promoter; positions of the –35, –10 elements and the transcription start site (+1) are indicated. (**B**) Analysis of the *in vivo* activity of the *rrnB* P1 promoter in the wild-type (WT) and I48S strains. (*Left*) Growth curves (OD_{600} values) for the WT (blue) and I48S (carmine) strains transformed with reporter plasmids containing the luciferase operon (*luxCDABE*) under the control of *rrnB* P1. (*Middle*) Analysis of luciferase activity at different stages of cell growth. At each time point, the luminescence intensity was normalized by the corresponding OD value (means and standard deviations from three biological replicates). (*Right*) The same data in log scale. (**C**) Effects of DksA and ppGpp on the activities of wild-type and I48S RNAPs on the plasmid template containing the *rrnB* P1 and RNA I promoters (positions of corresponding transcripts are indicated). (**D**) Quantification of data from (C). For each reaction point, the amount of the *rrnB* P1 transcript was divided by the amount of RNA I (means and standard deviations from four independent experiments). (**E**) Titration of DksA (upper panel) or DksA in the presence of ppGpp (200 μM; lower panel) for wild-type and mutant RNAPs. For each DksA concentration, the amount of transcript from the *rrnB* P1 promoter was divided by the amount of RNA I and normalized to the RNAP activity in the absence of DksA (means and standard deviations from 3 independent experiments).

binding, RNA priming or promoter escape. We therefore tested possible contributions of these factors to the activity of the I48S RNAP *in vitro*, using supercoiled and linear *rrnB* P1 templates. Titration experiments revealed similar dependency of the RNAP activity on the concentration of wild-type and I48S σ subunits suggesting that the mutation does not significantly change holoenzyme assembly (Supplementary Figure S5C). During the stationary phase, the RNAP σ^{70} holoenzyme becomes a target for the regulatory 6S RNA that binds within the DNA binding cleft of RNAP and inhibits its interactions with promoters, depending on the promoter complex stability (56,57). To test whether the I48S substitution could affect RNAP sensitivity to 6S RNA, we measured RNAP activities *in vitro* at various 6S RNA concentrations. WT and I48S RNAPs were similarly inhibited by 6S RNA on both unstable *rrnB* P1 and stable RNA I and T7A1 promoters (Supplementary Figure S5D and S5E), suggesting that both RNAP variants have similar sensitivities to 6S RNA.

Ribosomal RNA promoters were shown to be particularly sensitive to changes in the initiating NTP concentrations (67,68). We found that the activity of the WT and I48S RNAPs similarly depended on the concentration of initiating ATP (Supplementary Figure S5F and G). Interestingly, the apparent K_M values for ATP measured in the reaction of full-length RNA synthesis differed significantly at different reaction conditions, but remained comparable for both RNAP variants. In transcription buffer containing low monovalent salt concentration (40 mM KCl), $K_{M,app}$ for ATP was in the range of 1–3 μM for supercoiled plasmid DNA, 10–20 μM for linear DNA at 37°C and 100 μM for linear DNA at 22°C (Supplementary Figure S5F and G). In comparison, $K_{M,app}$ determined in previously published studies on supercolied DNA templates at higher salt con-

centrations was 10–20 μM at 100–150 mM KCl (32,69,69) and 250–300 μM at 150–170 mM KCl (67,68). Therefore, the composite $K_{M,app}$ values determined from full-length RNA synthesis greatly depend on the reaction conditions, and the observed differences may reflect changes in the stabilities of RNAP complexes with *rrnB* P1. At the same time, the I48S substitution does not significantly affect nucleotide binding in the active site of RNAP.

Since DNA melting during transcription initiation is a rapidly reversible step in the case of *rrnB* P1, changes in the stability of promoter complexes serve as an important regulatory mechanism that controls rRNA synthesis (49,60,62,63). We therefore compared promoter complex half-life times for wild-type and I48S RNAPs by incubating preformed promoter complexes with the polyanion heparin or competitor DNA (downstream fork-junction containing a -10-like motif), followed by measurements of residual RNAP activity (Figure 7A and B). To prevent transcription reinitiation in control reactions lacking competitors, NTP substrates were added together with heparin (in experiments with the heparin competitor) or rifapentine (in experiments with fork-junction DNA). Rifapentine blocks RNA extension past three nucleotides so that already formed promoter complexes can rapidly initiate RNA synthesis after rifapentine addition, while the next round of initiation is inhibited. As expected, the activity of the RNA I promoter that forms stable complexes with RNAP remained unchanged in the presence of competitors for both RNAPs during the course of experiments (Figure 7A and B). In contrast, the complexes of the WT RNAP with the *rrnB* P1 promoter rapidly dissociated in the presence of heparin, with half-life time ($t_{1/2}$) of ∼69 ± 5 s. The complexes of the mutant RNAP had an even lower stability ($t_{1/2}$ of 30 ± 4 s, ∼2-fold decrease relative to the WT RNAP) (Figure 7A and C, left). In the case of the downstream fork-junction competitor, the differences between the wild-type and mutant RNAPs became much more dramatic. The stability of promoter complexes formed by the mutant RNAP was comparable to the reactions with heparin (59 ± 14 s), while the lifetime of promoter complexes of WT RNAP much higher in comparison with heparin-containing reactions ($t_{1/2}$ of 1010 ± 230 s) (Figure 7B and C, right). Therefore, the dowstream fork-junction DNA competes with the full-length promoter more efficiently in the case of the mutant RNAP, suggesting that the mutation may affect RNAP interactions with the downstream promoter part during transcription initiation. Notably, the activity of the mutant RNAP on *rrnB* P1 was also decreased in control samples that were not incubated with competitors prior to NTP addition (compare Figure 7AB with Figure 6C), probably because in this case heparin or rifapentine present in the NTP mixture inhibited even the first round of transcription initiation from the unstable *rrnB* P1 promoter (i.e. a lower fraction of the mutant RNAP formed promoter complexes at the time of NTP addition). Together, these results demonstrate that the I48S substitution does not increase promoter complex stability but rather destabilizes RNAP–promoter interactions.

To test whether the mutation has any effects on RNAP-DNA interactions during transcription initiation, we performed footprinting of RNAP-*rrnB* P1 promoter complexes. To detect DNA melting in the open promoter complex, the samples were treated with potassium permanganate that modifies unpaired thymine residues in the melted promoter region, using a linear promoter DNA fragment. Previous studies demonstrated that efficient melting of *rrnB* P1 on linear DNA can only occur in the presence of initiating substrates, which stabilize the complex (62). We therefore added two initiating nucleotides, ATP and CTP, to the reaction mixtures. In agreement with published studies, the wild-type RNAP could melt the –10 element (with unpaired thymines detected at positions –13, –11 and –10 of the template strand), with only faint melting observed at position –3 near the transcription start site (Supplementary Figure S6A and S6B) (62). DksA suppressed DNA melting at all promoter positions. The patterns of thymine modifications for the I48S mutant was comparable to the wild-type RNAP both in the absence and in the presence of DksA (Supplementary Figure S6B).

We next probed the interactions of the WT and I48S RNAPs with downstream promoter DNA by Exo III footprinting. Exo III degrades the 3′-strand starting from the end of double-stranded DNA and can be used to detect the downstream border of RNAP on promoter DNA using a linear promoter fragment labeled at the 5′-end of the non-template strand (Supplementary Figure S6A and S6C). In the absence of NTP substrates, Exo III stops were detected at promoter positions from +15 to +18, for both WT and I48S RNAPs (Supplementary Figure S6C, top). In the presence of initiating NTPs allowing for synthesis of up to 5-mer RNA (CTP, UTP, GTP and a CpA primer), the downstream border detected by Exo III was shifted to position +22 at the initial time point of Exo III treatment and gradually moved back to position +15 after more prolonged incubation with Exo III for both RNAP variants, likely as a result of forward and backward oscillations of the initiating complex during abortive RNA synthesis (Supplementary Figure S6C, bottom). A somewhat weaker Exo III protection at position +22 observed for the I48S RNAP (compare lanes 3–5 and 9–11) may result from the decreased stability of initiating complexes formed by the mutant RNAP. At the same time, these experiments demonstrate that the overall geometry of RNAP-DNA interactions in the promoter complex remain similar for the wild-type and mutant RNAPs.

Changes in the stability of RNAP–promoter complexes may potentially affect the process of promoter escape by RNAP. To detect possible differences in the efficiency of promoter escape between the WT and I48S RNAPs, we measured the ratio of abortive and full-length RNA transcripts synthesized during transcription initiation from a T7A1cons promoter. In contrast to *rrnB* P1, whose initiating complexes with RNAP are unstable and produce very little amounts of abortive RNAs (70), the initiating complexes formed with T7A1cons are stable and produce large amounts of up to 16-mer abortive RNAs (2,3). The amounts of abortive RNAs synthesized by the mutant RNAP on this promoter were about two-fold lower than in the case of WT RNAP, suggesting that the I48S substitution may increase the rate of promoter escape or decrease the fraction of transcription initiation complexes engaged in abortive RNA synthesis (Figure 7D) (71).

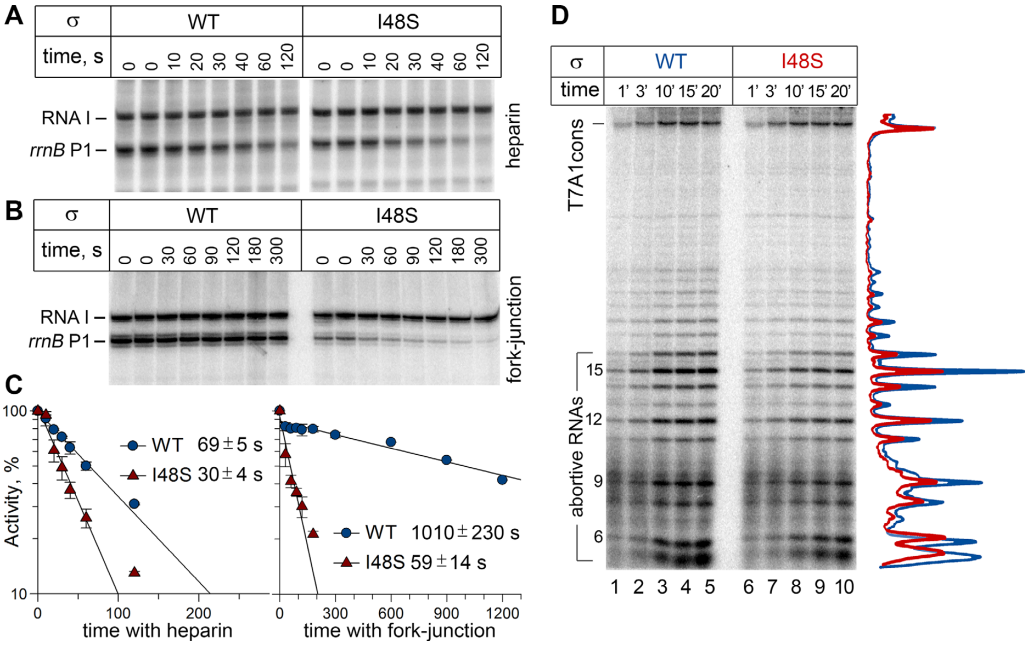

Figure 7. Effects of the I48S substitution on promoter complex stability and promoter escape by RNAP. (**A**) Measurements of promoter complex stabilities for the wild-type (WT) and I48S RNAPs in the presence of heparin. Preformed complexes of RNAP with plasmid templates were incubated with heparin for indicated time intervals (with two identical control samples incubated without competitor, '0'), followed by the addition of NTPs (and heparin to prevent transcription reinitiation in the control samples). Positions of the *rrnB* P1 and RNA I transcripts are indicated. (**B**) Measurements of promoter complex stabilities in the presence of the fork-junction DNA competitor. The reactions were performed similarly to (A) but the NTP mixture contained rifapentin. (**C**) Dissociation kinetics of the *rrnB* P1 promoter complex for WT and I48S RNAPs in the presence of heparin (left) or fork-junction DNA (right). For each time point, full-length RNA synthesis from *rrnB* P1 was normalized by RNAP activity in the control reactions and the data were fitted to a single-exponential equation (means and standard deviations from three independent experiments). (**D**) Analysis of the efficiency of promoter escape by RNAP. Transcription reactions were performed with either WT (blue) or I48S (red) RNAPs on the T7A1cons promoter template in the presence of all four NTPs, resulting in the synthesis of full-length and abortive (≤16 nt) RNA products. The transcription profiles for each RNAP are shown on the right.

DISCUSSION

σ^{70} is the major transcriptional regulator of *E. coli*, so it is not surprising that mutations in conserved regions of the σ factor, in particular those directly involved in interactions with DNA and core RNAP, can result in strong changes in promoter recognition and gene expression (1,9). In contrast, the functions of the highly variable region 1.1 in σ^{70} and other primary σs remain poorly understood. While it was previously shown that mutations in this region can change the stability and conformation of free σ and affect promoter recognition by the RNAP holoenzyme *in vitro* (12,17–20,72), their possible effects on transcription regulation *in vivo* have never been studied. We demonstrate that even a single amino acid substitution in region 1.1 in σ^{70} can significantly modulate the activity of RNAP leading to dramatic changes in gene expression and cell adaptation.

Our experiments revealed that the I48S substitution enhances RNAP activity on the *rrnB* P1 promoter, which controls transcription of one of rRNA operons in *E. coli*, both *in vitro* and *in vivo*. Ribosomal RNA promoters form unstable complexes with RNAP, which makes them susceptible to efficient inhibition by the stringent response factors, DksA and ppGpp (60,61). Unexpectedly, the mutation further destabilized intrinsically unstable RNAP-*rrnB* P1 complexes, but without reducing their activity. Similarly, substitutions G52A and D61A in region 1.1 were also shown to decrease promoter complex stability but their effects on *rrnB* P1 have not been tested (12). In contrast, deletion of region 1.1 was shown to strongly increase the stability of RNAP complexes with several tested promoters (20). Since promoter complexes formed by the I48S RNAP are particularly sensitive to competition with a downstream fork-junction DNA probe, it can be speculated that the mutation disrupts accommodation of the downstream promoter part by RNAP, either allosterically or through direct competition of region 1.1 with DNA (20).

The mutant RNAP also retains a higher level of activity on *rrnB* P1 in the presence of DksA and has a lower apparent affinity to DksA. This result is surprising because previous studies found a negative correlation between promoter complex stability and its apparent affinity to DksA (63). We propose that the I48S substitution may change the conformation and position of region 1.1 in the RNAP holoenzyme or in the open promoter complex and allosterically modulate DksA binding within the secondary channel of RNAP, thus making it more resistant to the DksA action. In particular, the I48S substitution may prevent DksA-dependent conformational changes in the β′ jaw and β lobe domains of RNAP, which were proposed to interfere with interactions with downstream DNA (63). This might also lead to changes in the conformation of the rim helixes bound by the C-terminal domain of DksA at the entry of the secondary channel (63) and reduce its affinity to RNAP.

A recently published study demonstrated that region 1.1 also plays a role in the regulation of transcription initiation

by another secondary channel factor, TraR (73). TraR is a small protein that binds RNAP in a similar way to DksA and mimics the combined action of DksA and ppGpp. It was proposed that TraR binding may destabilize the interaction between region 1.1 and the DNA binding cleft of RNAP, thus facilitating ejection of $\sigma^{70}_{1.1}$ during promoter binding. TraR (and by analogy DksA/ppGpp) may therefore lower the kinetic barrier between the closed and open promoter complexes, ultimately resulting in the decreased promoter complex stability. In the case of certain promoters, in which this barrier is rate limiting, this may lead to transcription activation (73). Structural changes in σ region 1.1 caused by the I48S substitution might also affect the kinetics of open complex formation, possibly explaining the observed effects of the I48S substitution on the activity of *rrnB* P1 and its regulation by DksA/ppGpp.

Destabilization of the RNAP–DNA interactions may in addition enhance promoter search by the mutant RNAP and increase RNAP turnover. It can also be proposed that changes in the promoter complex properties caused by the mutation might affect transcription by stimulating promoter escape by RNAP. Although this step is already highly efficient in the case of *rrnB* P1 promoter, we demonstrate that the ratio of abortive and productive transcripts is indeed decreased for the I48S RNAP in the case of the T7A1cons promoter that forms stable complexes with RNAP.

Furthermore, we demonstrated that the I48S substitution likely changes the conformation of free σ^{70} and enhances its interactions with promoter sequences. Similarly, previously studied deletions (13,15,58) and substitutions (including closely located A59G (72)) in region 1.1 were shown to affect σ-DNA interactions. Residue I48, which is located in one of the α helixes formed by region 1.1 (Figure 1B), is weakly conserved in primary σ factors but is often replaced with closely related amino acid residues, including leucine and valine (Figure 1A). Therefore, its substitution with a hydrophilic serine in the mutant σ factor may disrupt the native conformation of region 1.1 and its interactions with other regions of σ^{70}. While promoter binding regions in free σ^{70} are masked by region 1.1, the ability of an isolated σ factor to recognize promoters was revealed for σ^{A} and σ^{B} in *B. subtilis*, with possible implications for transcription regulation (74,75). It remains to be established whether unmasking of the DNA-binding domains of σ^{70} may also result in more efficient promoter recognition by the mutant RNAP.

Previously, it was proposed that the position and the functional role of σ region 1.1 may be different for different promoter complexes, depending on RNAP interactions with downstream DNA (20). Thus, mutations in this region may have differential effects on promoter activity at the genomic scale. Similarly, transcription factors, such as the gp2 protein of phage T7 (Figure 1C), can exploit interactions with region 1.1 for promoter-specific transcription regulation or RNAP inhibition (21). Indeed, transcriptome analysis revealed complex changes in gene expression in the I48S strain, which were more pronounced in the exponential stage of growth.

The pattern of enriched pathways among upregulated genes in the mutant strain has a distinct similarity with *ΔdksA* cells, with overlapped sets of differentially expressed genes in their transcriptomes (Figure 4A). The strains also have a similar phenotype of the extended lag phase, indicative of difficulties with adaptation to new environmental conditions (76,77). Although DksA is usually described as a regulator of stringent response, its expression levels are constant during exponential and stationary phases (78). Furthermore, published data suggest that it may act as a general transcription regulator (79) and help to prevent conflicts between transcription and replication (80) in the exponential phase of growth. For example, DksA was shown to take part in the transcriptional control of the *fis* gene, which encodes an essential regulator of growth promoting genes. In the absence of DksA, *fis* expression was significantly increased not only during transition to the stationary phase (since P*fis* is subjected to stringent response inhibition similarly to *rrnB* P1) but even during lag and exponential phases (52,79). Similarly, *fis* is 6-fold upregulated in the I48S cells collected in the exponential phase. Other examples of similarly regulated genes in the *ΔdksA* and I48S strains in the exponential phase include genes encoding rRNA, ribosomal proteins, flagella components, chemotaxis system, fatty acids biosynthesis pathway and multiple stress-response genes. The observed differential expression of genes controlled by the stringent response in the mutant strain may therefore be at least partially explained by the decreased sensitivity of I48S RNAP to DksA, which may mimic DksA deficiency in *ΔdksA* strains. At the same time, the amino acid biosynthesis pathway was significantly upregulated in the transcriptome of the I48S strain, although DksA is an activator of this pathway. Moreover, in contrast to the I48S strain the *ΔdksA* strain is unable to grow in minimal media without a specific set of amino acids (81), indicating that the properties of these two strains are not identical.

These observations highlight complex effects of the I48S mutation on bacterial physiology that may be caused by at least two independent mechanisms: the decreased sensitivity of I48S RNAP to DksA, and changes in the stabilities and activities of promoter complexes independent of the DksA function. As was shown by Galburt (82), the lowering of the kinetic barrier between closed and open complexes can result in activation of transcription for both stable and unstable promoter complexes by, which may be the case for the I48S RNAP (see above). This may result in simultaneous upregulation of multiple differentially regulated biosynthetic genes (rRNA and amino acids biosynthesis), as observed in the transcriptome of the I48S strain. At the same time, the observed changes in the expression of genes coding for alternative σ factors and other major transcription factors (Figure 4B, C) make it hard to distinguish between primary and secondary transcriptional effects of the I48S mutation. Furthermore, although less likely, changes in the expression level of some RNAs may be caused by their altered stability due to secondary effects caused by the I48S mutation.

Transcriptome changes in the mutant strain were less pronounced in the stationary phase than in actively growing cells, which could be explained by several reasons. Although the activity of I48S RNAP on the *rrnB* P1 promoter was higher compared to WT RNAP even in the presence of both ppGpp and DksA, their joint action resulted in a significantly higher level of inhibition in comparison to DksA

alone. Accordingly, the activity of the *rrnB* P1 reporter was strongly decreased in the stationary phase of growth even in the I48S cells (Figure 6B). Importantly, the levels of expression of both DksA and RelA/SpoT, responsible for ppGpp synthesis, were comparable for the wild-type and mutant strains during both exponentional and stationary growth (<2-fold difference; Supplement file 1 and 2). The intracellular concentration of ppGpp in stressed *E. coli* cells may be as high as 1–2 mM (83), so it may be speculated that saturating levels of ppGpp in combination with DksA are able to efficiently suppress transcription in the mutant strain. Still, stress-related genes were somewhat enriched among the downregulated genes, including well-known factors responsible for translation inhibition in the stationary phase (RMF, HPF, S22), which correlates with the increased rate of ongoing protein synthesis in stationary cells (Figure 2F). In addition, the activity of the σ^{70} RNAP holoenzyme in the stationary phase is suppressed by the anti-sigma factor Rsd and 6S RNA, which was shown to inhibit wild-type and I48S RNAPs with similar efficiencies (Supplementary Figure S5). However, it should be noted that the levels of 6S RNA were lower in the I48S strain compared to the WT strain in all analyzed phases of growth. These changes might partially explain higher levels of synthetic activity observed for the mutant strain.

Recently, the Palsson group proposed a model of 'Fear vs. Greed' tradeoff in transcription regulation (84). The 'Greed' modulon is enriched with genes required for bacteria growth, while the 'Fear' genes are responsible for stress response and survival (i.e. the RpoS regulon). The I48S cells exhibit a pronounced phenotype of decreased 'Fear' described by reduced activity of the RpoS regulon and increased expression of growth promoting genes in the exponential phase. This phenotype is further described by dysregulation of proper resource allocation during regrowth from the stationary phase resulting in a growth delay after dilution of cell culture with fresh medium. Indeed, our FACS data shows that the I48S cells activate their metabolism almost immediately after dilution with fresh medium.

The distinct shift of expression from stress-related to growth-promoting genes in the I48S strain results in a decreased number of dormant cells in the culture thus making it much more sensitive to environmental stress, such as antibiotic treatment. Although one would expect that the extended lag phase of the mutant strain should increase its tolerance to antibiotics (phenotype known as 'tolerance by lag' (74)) we have shown the opposite effect. This observation can be explained by the abnormal metabolic activity of the mutant strain, which differs from the generally accepted view of the lag phase metabolism. In the lag phase, metabolism of the wild-type strain is relatively low, while the mutant cells are described by a rapid increase of synthetic activity. This rapid activation results in dysregulation of proper resource allocation, leading to a prolonged lag phase, and makes the cells more susceptible to antibiotic treatment. One of the possible explanations for the observed delay is upregulation of ribosomal genes and translation, thus lowering the resources available for transcription of other genes required for active growth and adaptation to new environmental conditions. Indeed, it was shown (86) that *E. coli* strains with reduced rRNA synthesis (mutants with deletion of 1–6 out of 7 rrn operons) actually have an increased growth rate and survival under DNA stress conditions caused by incubation with ciprofloxacin or nalidixic acid.

In summary, our results suggest that the I48S mutation may rewire cellular transcription by modulating the strength of RNAP-promoter interactions and changing RNAP sensitivity to the stringent response factors, thus revealing previously unknown functions of σ region 1.1 in transcription regulation and stress adaptation. A distinct dysregulation of σ regulons in the I48S cells suggests that region 1.1 may also be involved in functional competition between the principal and alternative σ factors at different phases of growth. Furthermore, our observations together with published data of other research groups highlight possible functions of DksA in transcription regulation in the exponential phase of growth, independent of the stringent response. Finally, understanding of the complex interplay between σ factors and transcription regulators acting on bacterial RNAP may help to develop new antibacterial compounds disrupting these interactions and making the cells more sensitive to antibiotic action.

DATA AVAILABILITY

The RNA-seq and whole genome sequencing datasets generated in this study are available from BioProject under accession number PRJNA588714.

SUPPLEMENTARY DATA

Supplementary Data are available at NAR Online.

ACKNOWLEDGEMENTS

We thank Dr H. Mori, NIG, Japan for providing us with the knockout strain JW0836, Dr Fedor Subach for a plasmid encoding the FastFT protein, Dr Alexander Arutyunyan for help with CD spectra measurement and Dr Katsuhiko Murakami for helpful discussions.

FUNDING

Russian Science Foundation [17-14-01393 to A.K., transcription analysis *in vitro* and 19-14-00043 to P.S., phenotype analysis *in vivo*] (in part); Russian Foundation for Basic Research [18-34-20095 to D.E.]. Funding for open access charge: Russian Science Foundation.
Conflict of interest statement. None declared.

REFERENCES

1. Feklístov,A., Sharon,B.D., Darst,S.A. and Gross,C.A. (2014) Bacterial sigma factors: a historical, structural, and genomic perspective. *Annu. Rev. Microbiol.*, **68**, 357–376.
2. Kulbachinskiy,A. and Mustaev,A. (2006) Region 3.2 of the σ subunit contributes to the binding of the 3′-initiating nucleotide in the RNA polymerase active center and facilitates promoter clearance during initiation. *J. Biol. Chem.*, **281**, 18273–18276.
3. Pupov,D., Kuzin,I., Bass,I. and Kulbachinskiy,A. (2014) Distinct functions of the RNA polymerase σ subunit region 3.2 in RNA priming and promoter escape. *Nucleic Acids Res.*, **42**, 4494–4504.
4. Zhang,Y., Feng,Y., Chatterjee,S., Tuske,S., Ho,M.X., Arnold,E. and Ebright,R.H. (2012) Structural basis of transcription initiation. *Science*, **338**, 1076–1080.

5. Feklistov,A., Barinova,N., Sevostyanova,A., Heyduk,E., Bass,I., Vvedenskaya,I., Kuznedelov,K., Merkiene,E., Stavrovskaya,E., Klimasauskas,S. *et al.* (2006) A basal promoter element recognized by free RNA polymerase sigma subunit determines promoter recognition by RNA polymerase holoenzyme. *Mol. Cell*, **23**, 97–107.
6. Haugen,S.P., Berkmen,M.B., Ross,W., Gaal,T., Ward,C. and Gourse,R.L. (2006) rRNA promoter regulation by nonoptimal binding of sigma region 1.2: an additional recognition element for RNA polymerase. *Cell*, **125**, 1069–1082.
7. Barinova,N., Kuznedelov,K., Severinov,K. and Kulbachinskiy,A. (2008) Structural modules of RNA polymerase required for transcription from promoters containing downstream basal promoter element GGGA. *J. Biol. Chem.*, **283**, 22482–22489.
8. Haugen,S.P., Ross,W., Manrique,M. and Gourse,R.L. (2008) Fine structure of the promoter-sigma region 1.2 interaction. *Proc. Natl. Acad. Sci. U.S.A.*, **105**, 3292–3297.
9. Gruber,T.M. and Gross,C.A. (2003) Multiple sigma subunits and the partitioning of bacterial transcription space. *Annu. Rev. Microbiol.*, **57**, 441–466.
10. Iyer,L.M. and Aravind,L. (2012) Insights from the architecture of the bacterial transcription apparatus. *J. Struct. Biol.*, **179**, 299–319.
11. Murakami,K. (2015) Structural biology of bacterial RNA polymerase. *Biomolecules*, **5**, 848–864.
12. Bowers,C.W., McCracken,A. and Dombroski,A.J. (2000) Effects of amino acid substitutions at conserved and acidic residues within region 1.1 of Escherichia coli sigma(70). *J. Bacteriol.*, **182**, 221–224.
13. Dombroski,A.J., Walter,W.A., Record,M.T., Slegele,D.A. and Gross,C.A. (1992) Polypeptides containing highly conserved regions of transcription initiation factor σ70 exhibit specificity of binding to promoter DNA. *Cell*, **70**, 501–512.
14. Dombroski,A.J. (1997) Recognition of the -10 promoter sequence by a partial polypeptide of sigma70 in vitro. *J. Biol. Chem.*, **272**, 3487–3494.
15. Schwartz,E.C., Shekhtman,A., Dutta,K., Pratt,M.R., Cowburn,D., Darst,S. and Muir,T.W. (2008) A full-length group 1 bacterial sigma factor adopts a compact structure incompatible with DNA binding. *Chem. Biol.*, **15**, 1091–1103.
16. Callaci,S., Heyduk,E. and Heyduk,T. (1999) Core RNA polymerase from E. coli induces a major change in the domain arrangement of the σ70 subunit. *Mol. Cell*, **3**, 229–238.
17. Wilson,C. and Dombroski,A.J. (1997) Region 1 of σ70 is required for efficient isomerization and initiation of transcription by Escherichia coli RNA polymerase. *J. Mol. Biol.*, **267**, 60–74.
18. Gruber,T.M., Markov,D., Sharp,M.M., Young,B.A., Lu,C.Z., Zhong,H.J., Artsimovitch,I., Geszvain,K.M., Arthur,T.M., Burgess,R.R. *et al.* (2001) Binding of the initiation factor σ70 to core RNA polymerase is a multistep process. *Mol. Cell*, **8**, 21–31.
19. Bowers,C.W. (1999) A mutation in region 1.1of sigma sigma 70 affects promoter DNA binding by Escherichia coli RNA polymerase holoenzyme. *EMBO J.*, **18**, 709–716.
20. Ruff,E.F., Drennan,A.C., Capp,M.W., Poulos,M.A., Artsimovitch,I. and Record,M.T. (2015) E. coli RNA polymerase determinants of open complex lifetime and structure. *J. Mol. Biol.*, **427**, 2435–2450.
21. Bae,B., Davis,E., Brown,D., Campbell,E.A., Wigneshweraraj,S. and Darst,S.A. (2013) Phage T7 Gp2 inhibition of Escherichia coli RNA polymerase involves misappropriation of σ70 domain 1.1. *Proc. Natl. Acad. Sci. U.S.A.*, **110**, 19772–19777.
22. Mekler,V., Kortkhonjia,E., Mukhopadhyay,J., Knight,J., Revyakin,A., Kapanidis,A.N., Niu,W., Ebright,Y.W., Levy,R. and Ebright,R.H. (2002) Structural organization of bacterial RNA polymerase holoenzyme and the RNA polymerase-promoter open complex. *Cell*, **108**, 599–614.
23. Mekler,V., Minakhin,L. and Severinov,K. (2011) A critical role of downstream RNA polymerase-promoter interactions in the formation of initiation complex. *J. Biol. Chem.*, **286**, 22600–22608.
24. Molodtsov,V., Nawarathne,I.N., Scharf,N.T., Kirchhoff,P.D., Showalter,H.D.H., Garcia,G.A. and Murakami,K.S. (2013) X-ray Crystal Structures of the *Escherichia coli* RNA Polymerase in Complex with Benzoxazinorifamycins. *J. Med. Chem.*, **56**, 4758–4763.
25. Zuo,Y. and Steitz,T.A. (2015) Crystal structures of the E. coli transcription initiation complexes with a complete bubble. *Mol. Cell*, **58**, 534–540.
26. Miropolskaya,N., Ignatov,A., Bass,I., Zhilina,E., Pupov,D. and Kulbachinskiy,A. (2012) Distinct functions of regions 1.1 and 1.2 of RNA polymerase σ subunits from Escherichia coli and Thermus aquaticus in transcription initiation. *J. Biol. Chem.*, **287**, 23779–23789.
27. Datsenko,K.A. and Wanner,B.L. (2000) One-step inactivation of chromosomal genes in Escherichia coli K-12 using PCR products. *Proc. Natl. Acad. Sci. U.S.A.*, **97**, 6640–6645.
28. Subach,F.V., Subach,O.M., Gundorov,I.S., Morozova,K.S., Piatkevich,K.D., Cuervo,A.M. and Verkhusha,V.V. (2009) Monomeric fluorescent timers that change color from blue to red report on cellular trafficking. *Nat. Chem. Biol.*, **5**, 118–126.
29. Martin,M. (2011) Cutadapt removes adapter sequences from high-throughput sequencing reads. *EMBnet j.*, **17**, 10.
30. Bankevich,A., Nurk,S., Antipov,D., Gurevich,A.A., Dvorkin,M., Kulikov,A.S., Lesin,V.M., Nikolenko,S.I., Pham,S., Prjibelski,A.D. *et al.* (2012) SPAdes: A new genome assembly algorithm and its applications to single-cell sequencing. *J. Comput. Biol.*, **19**, 455–477.
31. Schindelin,J., Arganda-Carreras,I., Frise,E., Kaynig,V., Longair,M., Pietzsch,T., Preibisch,S., Rueden,C., Saalfeld,S., Schmid,B. *et al.* (2012) Fiji: an open-source platform for biological-image analysis. *Nat. Methods*, **9**, 676–682.
32. Pupov,D., Petushkov,I., Esyunina,D., Murakami,K.S. and Kulbachinskiy,A. (2018) Region 3.2 of the σ factor controls the stability of rRNA promoter complexes and potentiates their repression by DksA. *Nucleic Acids Res.*, **46**, 11477–11487.
33. Svetlov,V. and Artsimovitch,I. (2015) Purification of bacterial RNA polymerase: tools and protocols. *Methods Mol. Biol.*, **1276**, 13–29.
34. Kulbachinskiy,A., Mustaev,A., Goldfarb,A. and Nikiforov,V. (1999) Interaction with free beta' subunit unmasks DNA-binding domain of RNA polymerase sigma subunit. *FEBS Lett.*, **454**, 71–74.
35. Petushkov,I., Esyunina,D. and Kulbachinskiy,A. (2017) σ38-dependent promoter-proximal pausing by bacterial RNA polymerase. *Nucleic Acids Res.*, **45**, 3006–3016.
36. Petushkov,I., Esyunina,D., Mekler,V., Severinov,K., Pupov,D. and Kulbachinskiy,A. (2017) Interplay between σ region 3.2 and secondary channel factors during promoter escape by bacterial RNA polymerase. *Biochem. J.*, **474**, 4053–4064.
37. Kang,W.-K., Icho,T., Isono,S., Kitakawa,M. and Isono,K. (1989) Characterization of the generimK responsible for the addition of glutamic acid residues to the C-terminus of ribosomal protein S6 in Escherichia coli K12. *Molec. Gen. Genet.*, **217**, 281–288.
38. Baba,T., Ara,T., Hasegawa,M., Takai,Y., Okumura,Y., Baba,M., Datsenko,K.A., Tomita,M., Wanner,B.L. and Mori,H. (2006) Construction of Escherichia coli K-12 in-frame, single-gene knockout mutants: the Keio collection. *Mol. Syst. Biol.*, **2**, 2006.0008.
39. Pletnev,P.I., Nesterchuk,M.V., Rubtsova,M.P., Serebryakova,M.V., Dmitrieva,K., Osterman,I.A., Bogdanov,A.A. and Sergiev,P.V. (2019) Oligoglutamylation of E. coli ribosomal protein S6 is under growth phase control. *Biochimie*, **167**, 61–67.
40. Lewis,K. (2007) Persister cells, dormancy and infectious disease. *Nat. Rev. Microbiol.*, **5**, 48–56.
41. Keren,I., Kaldalu,N., Spoering,A., Wang,Y. and Lewis,K. (2004) Persister cells and tolerance to antimicrobials. *FEMS Microbiol. Lett.*, **230**, 13–18.
42. Roostalu,J., Jõers,A., Luidalepp,H., Kaldalu,N. and Tenson,T. (2008) Cell division in Escherichia coli cultures monitored at single cell resolution. *BMC Microbiol.*, **8**, 68.
43. Dewachter,L., Fauvart,M. and Michiels,J. (2019) Bacterial heterogeneity and antibiotic survival: understanding and combatting persistence and heteroresistance. *Mol. Cell*, **76**, 255–267.
44. Huang,D.W., Sherman,B.T. and Lempicki,R.A. (2009) Systematic and integrative analysis of large gene lists using DAVID bioinformatics resources. *Nat. Protoc.*, **4**, 44–57.
45. Szklarczyk,D., Gable,A.L., Lyon,D., Junge,A., Wyder,S., Huerta-Cepas,J., Simonovic,M., Doncheva,N.T., Morris,J.H., Bork,P. *et al.* (2019) STRING v11: protein–protein association networks with increased coverage, supporting functional discovery in genome-wide experimental datasets. *Nucleic Acids Res.*, **47**, D607–D613.
46. Paley,S., Parker,K., Spaulding,A., Tomb,J.-F., O'Maille,P. and Karp,P.D. (2017) The Omics Dashboard for interactive exploration of gene-expression data. *Nucleic Acids Res.*, **45**, 12113–12124.
47. Santos-Zavaleta,A., Salgado,H., Gama-Castro,S., Sánchez-Pérez,M., Gómez-Romero,L., Ledezma-Tejeida,D., García-Sotelo,J.S., Alquicira-Hernández,K., Muñiz-Rascado,L.J., Peña-Loredo,P. *et al.* (2019) RegulonDB v 10.5: tackling challenges to unify classic and

high throughput knowledge of gene regulation in *E. coli* K-12. *Nucleic Acids Res.*, **47**, D212–D220.
48. Lemke,J.J., Durfee,T. and Gourse,R.L. (2009) DksA and ppGpp directly regulate transcription of the Escherichia coli flagellar cascade: Regulation of the flagellar cascade by DksA/ppGpp. *Mol. Microbiol.*, **74**, 1368–1379.
49. Paul,B.J., Barker,M.M., Ross,W., Schneider,D.A., Webb,C., Foster,J.W. and Gourse,R.L. (2004) DksA: a critical component of the transcription initiation machinery that potentiates the regulation of rRNA promoters by ppGpp and the initiating NTP. *Cell*, **118**, 311–322.
50. Lemke,J.J., Sanchez-Vazquez,P., Burgos,H.L., Hedberg,G., Ross,W. and Gourse,R.L. (2011) Direct regulation of Escherichia coli ribosomal protein promoters by the transcription factors ppGpp and DksA. *Proc. Natl. Acad. Sci. U.S.A.*, **108**, 5712–5717.
51. My,L., Rekoske,B., Lemke,J.J., Viala,J.P., Gourse,R.L. and Bouveret,E. (2013) Transcription of the escherichia coli fatty acid synthesis operon fabHDG is directly activated by FadR and inhibited by ppGpp. *J. Bacteriol.*, **195**, 3784–3795.
52. Aberg,A., Fernandez-Vazquez,J., Cabrer-Panes,J.D., Sanchez,A. and Balsalobre,C. (2009) Similar and divergent effects of ppGpp and DksA deficiencies on transcription in escherichia coli. *J. Bacteriol.*, **191**, 3226–3236.
53. Paul,B.J., Berkmen,M.B. and Gourse,R.L. (2005) DksA potentiates direct activation of amino acid promoters by ppGpp. *Proc. Natl. Acad. Sci. U.S.A.*, **102**, 7823–7828.
54. Polikanov,Y.S., Blaha,G.M. and Steitz,T.A. (2012) How hibernation factors RMF, HPF, and YfiA turn off protein synthesis. *Science*, **336**, 915–918.
55. Izutsu,K., Wada,C., Komine,Y., Sako,T., Ueguchi,C., Nakura,S. and Wada,A. (2001) Escherichia coli ribosome-associated protein SRA, whose copy number increases during stationary phase. *J. Bacteriol.*, **183**, 2765–2773.
56. Burenina,O.Y., Elkina,D.A., Hartmann,R.K., Oretskaya,T.S. and Kubareva,E.A. (2015) Small noncoding 6S RNAs of bacteria. *Biochem. Mosc.*, **80**, 1429–1446.
57. Cavanagh,A.T. and Wassarman,K.M. (2014) 6S RNA, a global regulator of transcription in Escherichia coli, Bacillus subtilis, and beyond. *Annu. Rev. Microbiol.*, **68**, 45–60.
58. Callaci,S., Heyduk,E. and Heyduk,T. (1998) Conformational changes of Escherichia coli RNA polymerase sigma70 factor induced by binding to the core enzyme. *J. Biol. Chem.*, **273**, 32995–33001.
59. Young,B.A., Anthony,L.C., Gruber,T.M., Arthur,T.M., Heyduk,E., Lu,C.Z., Sharp,M.M., Heyduk,T., Burgess,R.R. and Gross,C.A. (2001) A coiled-coil from the RNA polymerase beta' subunit allosterically induces selective nontemplate strand binding by sigma(70). *Cell*, **105**, 935–944.
60. Gourse,R.L., Chen,A.Y., Gopalkrishnan,S., Sanchez-Vazquez,P., Myers,A. and Ross,W. (2018) Transcriptional Responses to ppGpp and DksA. *Annu. Rev. Microbiol.*, **72**, 163–184.
61. Paul,B.J., Ross,W., Gaal,T. and Gourse,R.L. (2004) rRNA transcription in Escherichia coli. *Annu. Rev. Genet.*, **38**, 749–770.
62. Rutherford,S.T., Villers,C.L., Lee,J.-H., Ross,W. and Gourse,R.L. (2009) Allosteric control of Escherichia coli rRNA promoter complexes by DksA. *Genes Dev.*, **23**, 236–248.
63. Molodtsov,V., Sineva,E., Zhang,L., Huang,X., Cashel,M., Ades,S.E. and Murakami,K.S. (2018) Allosteric effector ppGpp potentiates the inhibition of transcript initiation by DksA. *Mol. Cell*, **69**, 828–839.
64. Ross,W., Sanchez-Vazquez,P., Chen,A.Y., Lee,J.-H., Burgos,H.L. and Gourse,R.L. (2016) ppGpp binding to a site at the RNAP-DksA interface accounts for its dramatic effects on transcription initiation during the stringent response. *Mol. Cell*, **62**, 811–823.
65. Ross,W., Vrentas,C.E., Sanchez-Vazquez,P., Gaal,T. and Gourse,R.L. (2013) The magic spot: a ppGpp binding site on E. coli RNA polymerase responsible for regulation of transcription initiation. *Mol. Cell*, **50**, 420–429.
66. Perederina,A., Svetlov,V., Vassylyeva,M.N., Tahirov,T.H., Yokoyama,S., Artsimovitch,I. and Vassylyev,D.G. (2004) Regulation through the secondary channel–structural framework for ppGpp-DksA synergism during transcription. *Cell*, **118**, 297–309.
67. Gaal,T., Bartlett,M.S., Ross,W., Turnbough,C.L. and Gourse,R.L. (1997) Transcription regulation by initiating NTP concentration: rRNA synthesis in bacteria. *Science*, **278**, 2092–2097.
68. Barker,M.M. and Gourse,R.L. (2001) Regulation of rRNA transcription correlates with nucleoside triphosphate sensing. *J. Bacteriol.*, **183**, 6315–6323.
69. Bartlett,M.S., Gaal,T., Ross,W. and Gourse,R.L. (1998) RNA polymerase mutants that destabilize RNA polymerase-promoter complexes alter NTP-sensing by rrn P1 promoters. *J. Mol. Biol.*, **279**, 331–345.
70. Winkelman,J.T., Chandrangsu,P., Ross,W. and Gourse,R.L. (2016) Open complex scrunching before nucleotide addition accounts for the unusual transcription start site of E. coli ribosomal RNA promoters. *Proc. Natl. Acad. Sci. U.S.A.*, **113**, E1787–E1795.
71. Sen,R., Nagai,H. and Shimamoto,N. (2000) Polymerase arrest at the lambdaP(R) promoter during transcription initiation. *J. Biol. Chem.*, **275**, 10899–10904.
72. Gopal,V. and Chatterji,D. (1997) Mutations in the 1.1 subdomain of escherichia coli sigma factor sigma70 and disruption of its overall structure. *Eur. J. Biochem.*, **244**, 613–618.
73. Chen,J., Gopalkrishnan,S., Chiu,C., Chen,A.Y., Campbell,E.A., Gourse,R.L., Ross,W. and Darst,S.A. (2019) E. coli TraR allosterically regulates transcription initiation by altering RNA polymerase conformation. *eLife*, **8**, e49375.
74. Kuo,H.-H., Huang,W.-C., Lin,T.-F., Yeh,H.-Y., Liou,K.-M. and Chang,B.-Y. (2015) The core-independent promoter-specific binding of *Bacillus subtilis* σ^{B}. *FEBS J.*, **282**, 1307–1318.
75. Yeh,H.-Y., Chen,T.-C., Liou,K.-M., Hsu,H.-T., Chung,K.-M., Hsu,L.-L. and Chang,B.-Y. (2011) The core-independent promoter-specific interaction of primary sigma factor. *Nucleic Acids Res.*, **39**, 913–925.
76. Rolfe,M.D., Rice,C.J., Lucchini,S., Pin,C., Thompson,A., Cameron,A.D.S., Alston,M., Stringer,M.F., Betts,R.P., Baranyi,J. *et al.* (2012) Lag phase is a distinct growth phase that prepares bacteria for exponential growth and involves transient metal accumulation. *J. Bacteriol.*, **194**, 686–701.
77. Gamba,P., James,K. and Zenkin,N. (2017) A link between transcription fidelity and pausing *in vivo*. *Transcription*, **8**, 99–105.
78. Edwards,A.N., Patterson-Fortin,L.M., Vakulskas,C.A., Mercante,J.W., Potrykus,K., Vinella,D., Camacho,M.I., Fields,J.A., Thompson,S.A., Georgellis,D. *et al.* (2011) Circuitry linking the Csr and stringent response global regulatory systems: Csr and stringent response systems. *Mol. Microbiol.*, **80**, 1561–1580.
79. Mallik,P., Paul,B.J., Rutherford,S.T., Gourse,R.L. and Osuna,R. (2006) DksA is required for growth phase-dependent regulation, growth rate-dependent control, and stringent control of fis expression in escherichia coli. *J. Bacteriol.*, **188**, 5775–5782.
80. Tehranchi,A.K., Blankschien,M.D., Zhang,Y., Halliday,J.A., Srivatsan,A., Peng,J., Herman,C. and Wang,J.D. (2010) The transcription factor DksA prevents conflicts between DNA replication and transcription machinery. *Cell*, **141**, 595–605.
81. Vinella,D., Potrykus,K., Murphy,H. and Cashel,M. (2012) Effects on growth by changes of the balance between GreA, GreB, and DksA suggest mutual competition and functional redundancy in Escherichia coli. *J. Bacteriol.*, **194**, 261–273.
82. Galburt,E.A. (2018) The calculation of transcript flux ratios reveals single regulatory mechanisms capable of activation and repression. *Proc. Natl Acad. Sci. U.S.A.*, **115**, E11604–E11613.
83. Varik,V., Oliveira,S.R.A., Hauryliuk,V. and Tenson,T. (2017) HPLC-based quantification of bacterial housekeeping nucleotides and alarmone messengers ppGpp and pppGpp. *Sci. Rep.*, **7**, 11022.
84. Sastry,A.V., Gao,Y., Szubin,R., Hefner,Y., Xu,S., Kim,D., Choudhary,K.S., Yang,L., King,Z.A. and Palsson,B.O. (2019) The *Escherichia coli* transcriptome mostly consists of independently regulated modules. *Nat Commun.*, **10**, 5536.
85. Fridman,O., Goldberg,A., Ronin,I., Shoresh,N. and Balaban,N.Q. (2014) Optimization of lag time underlies antibiotic tolerance in evolved bacterial populations. *Nature*, **513**, 418–421.
86. Bollenbach,T., Quan,S., Chait,R. and Kishony,R. (2009) Nonoptimal microbial response to antibiotics underlies suppressive drug interactions. *Cell*, **139**, 707–718.